PERFORMANCE ASSESSMENT OF A BPSK CDMA SYSTEM USING AN URBAN RADIO CHANNEL MODEL

A Master's Thesis
Presented by
Alime YANARTAŞ

to
the Graduate School of Natural and Applied Sciences
of Middle East Technical University
in Partial Fulfillment for the Degree of

MASTER OF SCIENCE

in

ELECTRICAL AND ELECTRONICS ENGINEERING

MIDDLE EAST TECHNICAL UNIVERSITY
ANKARA
December, 1991

Approval of the Graduate School of Natural and Applied Sciences.

R. Sever

for Prof. Dr. Alpay Ankara
Director

I certify that this thesis satisfies all the requirements as a thesis for the degree of Máster of Science.

Prof. Dr. Tuncay Birand
Chairman of the Department

We certify that we have read this thesis and that in our opinion it is fully adequate, in scope and quality, as a thesis for the degree of Master of Science in Electrical and Electronics Engineering.

Prof. Dr. Yalçın Tanık
Supervisor

Examining Committee in Charge:
Prof. Dr. Rüyal Ergül (Chairman)
Prof. Dr. Yalçın Tanık
Prof. Dr. Canan Toker
Asst. Prof. Dr. Sencer Koç
Levent Aydoğan, M.S.E.E. (ASELSAN)

ABSTRACT

PERFORMANCE ASSESSMENT OF A BPSK CDMA SYSTEM USING AN URBAN RADIO CHANNEL MODEL

YANARTAŞ, Alime

A MSc Thesis in Electrical and Electronics Engineering

Supervisor: Prof. Dr. Yalçın TANIK

December, 1991, 99 pages

In this thesis, a transmission system which uses BPSK and direct sequence spreading is considered. For a given set of channel parameters , the probability of bit error is derived and obtained by considering the effects of AWGN, spreading sequence and the estimation error of the channel parameters. The Suzuki-Hashemi channel model is used in simulations. The receiver is based on a RAKE structure which is implemented with the maximal ratio combiner using the estimated channel parameters as its weights.Perfect synchronization is assumed in analyses. Many simulation runs have been performed to assess the performance of the system under several operating conditions : Combinations of different E_b / N_o, RF bandwidth, bit rate, perfect and slow power control cases, Doppler spread, number of taps of the RAKE receiver were considered. Using these conditions, the capacity of CDMA is calculated.

Keywords: Mobile Communications, Spread Spectrum, CDMA, Multipath Fading Channels, Diversity Combining, RAKE Receiver

Science Code: 6090207.

ÖZ

BİR İKİLİ - FAZ - KAYDIRMA - ANAHTARLI KOD- BÖLMELİ-ÇOKLU-ERİŞİM SİSTEMİNİN KENTSEL BİR RADYO KANAL MODELİ KULLANILARAK BAŞARIM DEĞERLENDİRİMİ

YANARTAŞ, Alime
Yüksek Lisans Tezi, Elektrik ve Elektronik Mühendisliği Anabilim Dalı
Tez Yöneticisi: Prof.Dr. Yalçın TANIK
Aralık, 1991, 99 sayfa

Bu tezde, İkili-Faz-Kaydırma-Anahtarlama ve doğrudan-dizi yayılım kullanan bir iletim sistemi ele alınmıştır. İkil hatası olasılığı, verilen bir kanal parametresi kümesi için türetilmiştir. Bu türetimde toplanır beyaz Gauss gürültüsünün, yayılım dizisinin ve kanal parametrelerindeki kestirim hatalarının etkileri de göz önüne alınmıştır. Benzetimlerde Suzuki-Hashemi kanal modeli kullanılmıştır. Alıcı, RAKE yapısı üzerine kurulmuştur. Bu yapı, kestirilmiş kanal parametrelerini ağırlıkları olarak kullanan bir en büyük oran birleştiricisiyle gerçekleştirilmiştir. Çözümlemelerde, kusursuz eşzamanlama varsayılmıştır. Sistemin bazı işletim koşullarındaki başarımını değerlendirmek için bir çok benzetim yapılmıştır. Bu koşullar şunlardır: Değişik E_b/N_o, RF bant genişliği, ikil dizi hızı, Doppler yayılımı, RAKE alıcısının uzunluğu, kusursuz ve yavaş güç denetimi durumlarının birleşileri. Bu koşullar kullanılarak Kod-Bölmeli-Çoklu-Erişimin sığası hesaplanmıştır.

Anahtar Kelimeler: Mobil İletişim, Yayılmış-İzge,Kod-Bölmeli-Çoklu-Erişim, Çok Yollu Sönümlü Kanallar, Başkalıklı-Katışım, RAKE alıcısı.

Bilim Dalı Sayısal Kodu: 6090207

ACKNOWLEDGEMENTS

The author would like to thank Prof. Dr. Yalçın Tanık for his excellent supervision and constructive criticism in the development of this thesis.

The author also wishes to express her sincere gratitude to Prof. Dr. Rüyal Ergül and Asst. Prof. Dr. Sencer Koç for their extensive help in the completion of this work.

Special thanks are due to Res. Asst. Yaşar Özüm, Res. Asst. Hacer Kapıdere, Res. Asst. Tulga Turna and Mr. Ali Türker for their help in writing this manuscript and their patience and encouragement.

The author also likes to express her deep gratitude to her parents for their moral and financial support throughout her life, and for encouraging her to pursue a higher education.

TABLE OF CONTENTS

LIST OF TABLES

LIST OF FIGURES

LIST OF SYMBOLS

AWGN	Additive White Gaussian Noise
AMPS	Advanced Mobile Phone System
BPSK	Binary Phase Shift Keying
CDMA	Code Division Multiple Access
DS	Direct Sequence
FDMA	Frequency Division Multiple Access
FEC	Forward Error Correction
FH	Frequency Hopping
FH/DS	Frequency Hopping / Direct Sequence
GMSK	Gaussian Minimum Shift Keying
GSM	Special Mobile Group
MRC	Maximal Ratio Combiner
MTSO	Mobile Telephone Switching Office
PN	Pseudorandom
QPSK	Quadrature Phase Shift Keying
SNR	Signal-to-Noise Ratio
SS	Spread Spectrum
ss	Spreading Sequence
TDMA	Time Division Multiple Access

CHAPTER I

INTRODUCTION

The design objective for mobile communication systems is primarily to achieve the highest user density at a specified reliability, usually given in terms of probability of blocking. In order to achieve this aim and to overcome the operational limitations of conventional mobile telephone systems such as limited service capability, poor service performance and inefficient frequency spectrum utilization, cellular mobile communication systems have been developed. In cellular systems, the allocated frequency band is reused in different geographic locations. As the number of cellular subscriber increases, interferences will also increase. Since digital signals are quite resistant to noise and interference as compared to analog signals, the trend is towards digital. As the population increases rapidly and very large scale integrated circuit (VLSI) digital signal processing replaces the bulky analog radio equipment, the demand for mobile radio communications gets higher and higher. In order to meet this demand (increased capacity of system), to improve quality and to enlarge the range of applications such as text, video, etc., various systems have been proposed in mobile communications. There are a number of other more important aspects of mobile communications that need to be mentioned. As less and less bandwidth per user becomes available, depending on the technique used, problems such as intersymbol interference (ISI), fading, etc., become more pronounced.

Mobile radio systems suffer from multipath fading which occurs due to the reflection and scattering of the electromagnetic waves by buildings and other obstacles. This multipath fading degrades the performance of the system. However, if the multipath medium is well characterized, the effect of this disturbance will be reduced significantly by choosing a suitable radio access technique.

Fading multipath channels can offer improved performance over flat fading (non-time-dispersive) channels because of the inherent diversity available from receiving the signal over multiple paths with different delays. A method for obtaining diversity is based on the use of a signal having a bandwidth much greater than the coherence bandwidth of the channel. Such a signal will resolve the multipath components and thus provide the receiver with several independently fading signal paths. Some multipath receivers have been designed to take advantage of resolvable paths. RAKE receiver is one of them and is known as the optimum receiver for processing wideband signals [9].

Spread spectrum (SS) techniques [9] are known to be quite resistant to fading and multipath effects due to the implicit diversity capability which becomes more pronounced as the bandwidth increases well above the coherence bandwidth of the channel. As mentioned earlier, in mobile communications, the channel characteristic is quite unfavourable because of time dispersion and multipath fading. Therefore, it is necessary to apply some methods to overcome these disturbances. CDMA (code division multiple access) is an efficient way of achieving this goal, and recently there has been considerable interest on the subject [6,12,13,14,18].

In the literature, there have been many studies which analyse various aspects of spread spectrum systems: Modulation methods, the effects of the spreading sequence and the additive white Gaussian noise (AWGN) on the probability of error, estimation of channel parameters, synchronization issues, etc. [5,6,8,9,10,13,15,28].

Multipath fading channels are characterized as having randomly time varying impulse responses. In the literature, many dynamic channel models can be found [1,3,7,9,11,21]. Among these Suzuki's [3,4] and Hashemi's [1,2] models for outdoor applications and Saleh's [11] indoor model can be cited. The impulse response of these channels consists of random pulses which are correlated both in time and delay variables. However, in many works done on the subject, the pulse variations corresponding to the propagation paths are assumed to be independent, Rayleigh processes [21]. Although there have been some studies based on simulations which take the correlation effect into account, they are limited to some specific cases [5,6]. Therefore, in order to investigate the effects of a certain channel on the characteristics of communications, we analysed BPSK modulation by using Hashemi-Suzuki channel model in this work. This choice is justified by the fact that

this particular channel model fits very well to the experimental outcomes, at least the specific area where the measurements were made [1,2].

This thesis presents results on the performance of a RAKE receiver with binary phase shift keying (BPSK) modulation. For a given set of channel parameters (path phasors) the probability of bit error (P_b) is obtained analytically by taking the effects of AWGN, the spreading sequence, and the estimation error of the channel parameters in to account. Next, a sequence of channel impulse responses (profiles) are generated by using the Suzuki-Hashemi simulation procedure and for each profile the corresponding ($P_{b)}$ is calculated. Thus P_b of the receiver is simulated as a function of the displacement of the mobile.

The outline of the thesis is as follows:

Chapter 2 consists of three major parts. First, the general nature of a mobile communication system is reviewed. Second, the basic features of cellular mobile systems are described. Finally, three fundamentally different ways to access and share a common channel resource are investigated:

1. Frequency Division Multiple Access (FDMA)
2. Time Division Multiple Access (TDMA)
3. Code Division Multiple Access (CDMA)

Chapter 3 covers the general aspects of spread spectrum systems. The capacity formula for CDMA systems is given in this chapter. In addition, the advantages and disadvantages of CDMA spread spectrum systems over TDMA and FDMA are briefly discussed.

Chapter 4 is concerned with the channel model used in the simulation [1,2]. This chapter is devoted to the method of simulation of the arrival times $\{t_k\}$, path amplitudes $\{a_k\}$, and the phase sequence $\{\theta_k\}$.

Chapter 5 is composed of two main sections. In the first section, the transmission system and its model are described. The probability of error analysis is carried out in the second section.

Chapter 6 presents simulations and performance results based on the theoretical probability of error derived in Chapter 5. The bit error performance is investigated in various aspects: perfect power control and slow power control, different RF bandwidths, bit rates, SNR, Doppler spread, number of taps of the RAKE receiver.

In the last chapter, conclusions are given.

The simulation program is listed in Appendix B.

A summary of this work can be found in [30].

CHAPTER II

MOBILE COMMUNICATION SYSTEM

2.1 Introduction

A conventional mobile telephone system is usually designed by selecting one or more channels from a specific frequency allocation for use in autonomous geographic areas. The communication coverage area of each zone is normally planned to be as large as possible. It means that the transmitter power should be very high. In a conventional mobile telephone system the mobile user calling in one zone has to reinitiate the call while moving into a new zone because the call will be dropped. This is an undesirable characteristics for a radio telephone system since a call may not be completed without a handoff capability. Handoff is a process of automatically varying frequencies as the mobile unit moves into a different frequency zone. Thus a call can be continued in a new zone without redialing. Another disadvantage of the conventional system is that the number of the active users is limited to the number of channels assigned to a specific frequency zone.

Considering frequency spectrum utilization, the conventional system does not use the spectrum efficiently since each channel can serve one user at a time in a whole area.

A major problem in radio communication industry is the limitation of available frequency band. As the population increases, the demand for mobile radio gets higher and higher. Therefore, a new system that will operate within a limited assigned frequency band and will serve an almost unlimited number of users in unlimited areas is needed.

Since microprocessors and minicomputers are used for controlling many complicated features and functions with less power and size, they provide possibilities to develop advanced mobile telephone systems.

According to the reasons discussed above, cellular mobile telephone systems have been developed. In the following section the basic features of cellular systems will be introduced.

2.2 Cellular Systems

2.2.1 Basic Cellular System

A basic cellular system is composed of four parts: a mobile unit, a cell site, a mobile telephone switching office (MTSO) and connections [23]. Fig. 2.1 shows a basic cellular system.

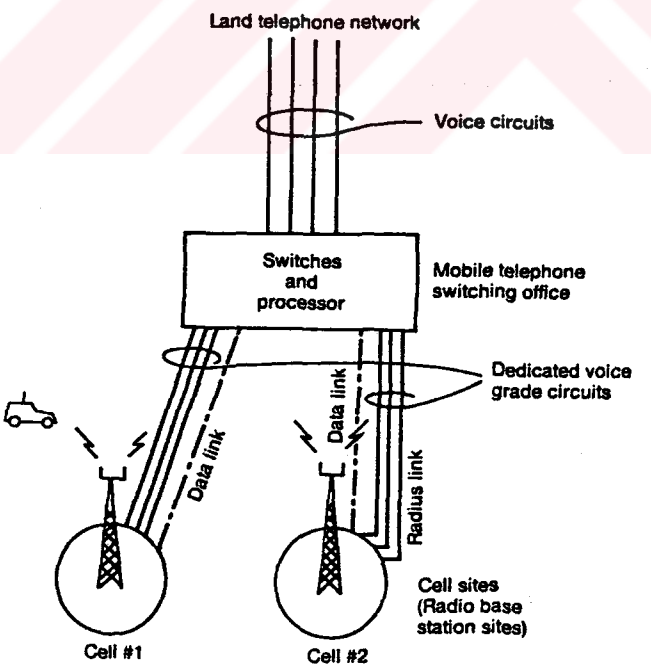

Figure 2.1. Basic Cellular System

1. Mobile Units : A mobile unit consists of a control unit, a transceiver, and an antenna system.

2. Cell Site : The cell site contains a control unit, radio cabinets, a power plant, and data terminals. Additionally, performance call supervision, mobile location, handoffs, and call termination are managed.

3. MTSO : The switching office , the central coordinating element for all cites, consists of the cellular processor and cellular switch. It interfaces with telephony zone offices, controls call processing, and handles billing activities.

4. Connections: The radio and high-speed data links connect the three subsystems. Each mobile unit can only use one channel at a time for its communication link. However, the channel is not fixed: it can be any one in the whole band assigned by the serving area, and each site has multichannel capabilities that can connect simultaneously to many mobile units.

The MTSO is the most important part of the cellular system. Its processor provides central coordination and cellular administration.

The cellular switch, which can be either analog or digital, switches calls to connect mobile users to other mobile users. It uses voice trunks similar to telephony interoffice trunks. It also contains data links that provides supervision links between the processor and the switch , and between the cell sites and processor. The radio link carries the voice and signalling between the mobile unit and the cell site. The high speed data cannot be transmitted over the standard telephone trunks. Therefore either microwave links or T-carriers (wire lines) that carry both voice and data between the cell site and the MTSO, must be used.

2.2.2 Performance Criteria

There are some categories for specifying performance criteria such as voice activity, and service quality. Only service quality is introduced in this section.

Three items are required for service quality.

1. Coverage

The system should serve as large area as possible, however, due to irregular geographic distributions, it is usually not practical to cover 100 percent of the area for two reasons:

a) The transmitter power would have to be very high to compensate for changes in signal level due to path loss variations and fading. The higher power results in a significant added cost factor.

b) The higher the transmitted power, the harder it becomes to control interference.

2. Required Grade of Service

For a normal start-up system, the grade of service is specified for a blocking probability of call initiation at the busy hour. In order to decrease the blocking probability a good system plan and a sufficient number of radio channels are required.

3. Number of Dropped Calls

During Q calls in an hour, if P call is dropped and (Q-P) calls are completed, then the call drop rate is P/Q. A low drop rate is desired. The coverage and handoff problems related to insufficient channel availability could cause a high drop rate.

2.2.3 Operation of Cellular Systems

This section briefly describes the operation of the cellular mobile system. that is explained in [23]. The operation can be divided into five parts.

1. Mobile Unit Initialization

When the user turns on the mobile station, the initialization work starts. The customer must scan all the channels and find an unoccupied one to use. The user selects the strongest set-up channel. This usually means selecting the nearest cell site. The set-up channels are used only for initiating or setting up phone calls. They can be classified by usage into two types : access channel and paging channels. The first type is used for the mobile originating calls and the second channels for the base station originating calls.

2. Mobile Originated Call

The user places the called number into an originating register in the mobile unit, checks to see that the number is correct. Then the customer pushes 'send' button. The cell site receives it, and then selects the best antenna for the voice channel to use. At the same time the cell site sends a request to the MTSO via high-speed data link. The MTSO selects a suitable voice channel for the call and connects the wire line party through the telephony zone office.

3. Network Originated Call

A land line party dials a mobile unit number. When a mobile call is received from a mobile number, the telephone company zone office, recognizing this,

forwards the call to the MTSO. The MTSO sends a paging message to certain cell sites based on the mobile unit number and the search algorithm.

Each cell site transmits the page on its own set-up channel. The mobile unit recognizes its own identification on a strong set-up channel, and locks onto it. Then it responds to the cell site. The mobile unit also follows the instruction to tune to an assigned voice channel and initiate user alert.

4. Call Termination

When the mobile user wants to terminate a call, a particular signal is transmitted to the cell site, and both sides let the voice channel free.

5. Handoff Procedure

When the mobile unit moves out of the coverage area of a specific cell site, the reception becomes weak. The present cell site needs a handoff. The system switches the call to a new frequency channel in a new cell site. During the process, the call continues without interrupting the call or alerting the user.

2.2.4 Cell Shapes

It has to be realized that the commonly used hexagonal-shaped communication cells are artificial and that such a shape cannot be generated in the real world. Engineers draw hexagonal-shaped cells to simplify the planning and design of a cellular system because it approaches a circular shape that is the ideal power coverage area. The ideal cell, the real cell, and the hexagonal cell shapes are shown in Fig. 2.2. Since the circular shapes have overlapped areas, it makes the drawing unclear. The hexagonal-shaped cells fit the area nicely with no gap and no overlap between cells.

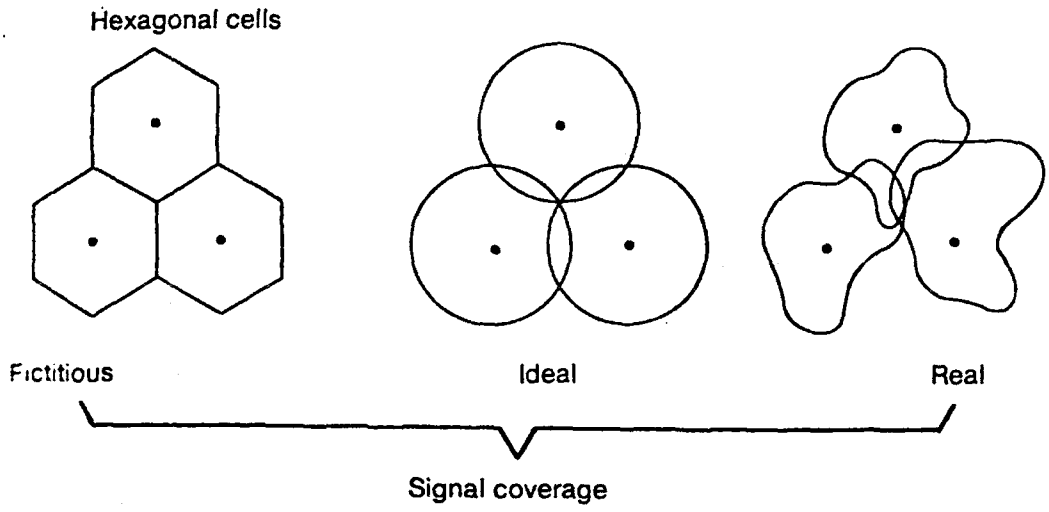

Figure 2.2. Cell Shapes

2.2.5 Frequency Reuse

Frequency reuse is the core concept of the cellular mobile radio system. Each cell has a fixed number of radio channels. When the cells are suitably separated geographically, users in different cells can simultaneously use the same frequency channel. This is called frequency reuse. The frequency reuse system can drastically increase the capacity or the spectrum efficiency since the transmitters are distributed with moderate power throughout the coverage area instead of covering a complete area from one transmitter site with high power. However, if the system is not properly designed, severe interference may occur. Interference due to use of the same channel is called co-channel interference. In order to combat this effect and to evaluate the system performance, frequency reuse distance D can be described. It is the minimum distance that allows the same frequency to be reused. The frequency reuse distance is a function of many factors such as the number of co-channel cells in the vicinity of the center cell, the antenna head, the transmitted power at cell site, and the propagational aspects of the geographic area.

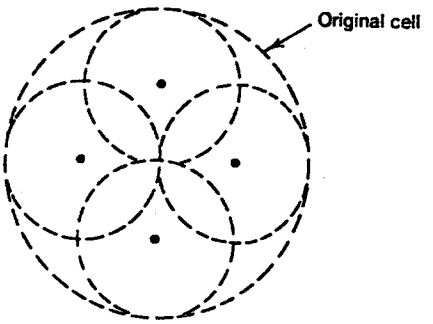

Figure 2.3. Cell Splitting

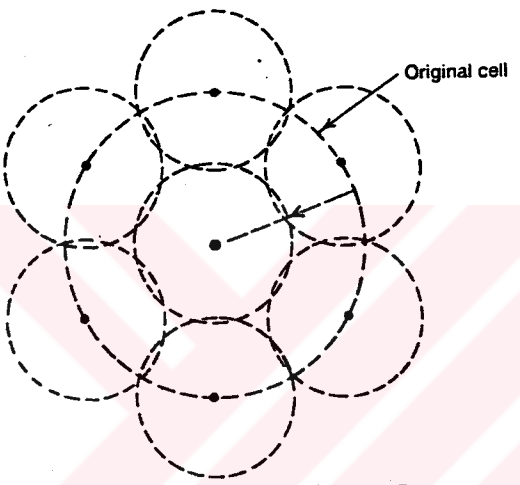

Figure 2.4. Cell Splitting

2.2.6 Cell Splitting

The cell splitting is the second concept to improve the utilization of spectrum efficiency. As mentioned earlier, each cell has a fixed number of channels whereas when the user density starts to increase and the frequency channels in each cell cannot provide enough mobile calls, the cell can be divided into smaller cells. This process is called cell splitting. There are two ways of splitting : In Fig. 2.3, the original cell site is not used, while in Fig. 2.4, it is.

2.2.7 Existing Cellular Systems

Looking at today's cellular products, we find many different cellular systems employed in different parts of the world. Some of them will be given below [Lee], and some features of them are in Table 2.1.

Japan: Nippon Telegraph and Telephone Corporation (NTT) developed an 800 MHz land mobile system. Then, the system was improved in 1985. The 1985 system operated over a spectrum of 30 MHz. At present, there is no competitive situation set up by the government.

Canadian System: In 1978, a system called AURORA was designed for the Alberta government telephone (AGT). It is a 400 MHz system. On-going developmental work on the AURORA is underway at 800 MHz.

Nordic System: This system was built mostly by Scandinavian countries (Denmark, Norway, Sweden and Finland) in cooperation with Saudi Arabia and Spain. It provides mobile telephone service at 450 MHz and is called the NMT network. NMT 900 MHz has been used since 1987.

Other European Cellular Systems:

The present cellular systems of Europe are as follows:

Benelux Country Network: In Netherland, ATF2 networks (the same as the NMT 450 network) are used. Ericsson AXE-10 switching network serves Luxembourg and Belgium.

United Kingdom: In 1982, two competing national cellular radio networks were announced. The UK system is called TACS (Total Access Communications System). Cellnet and Vodafone systems are operating at 900 MHz in the United Kingdom.

Table 2.1 Examples of Cellular Phones Used in the World.

	Japan	North America	England	Scandinavia	Germany
	NTT	AMPS	TACS	NMT	C450
Transmision Frequency (MHz)					
Base Station	870 - 885	870 - 890	935 - 960	463 - 467.5	461.3-465.74
Mobile Station	925 - 940	825 - 845	890 - 915	453 - 457.5	451.3-455.74
Spacing Between Channels (KHz)	25	30	25	25	20
Audio Signal: Modulation	FM	FM	FM	FM	FM
Control Signal: Modulation	FSK	FSK	FSK	FSK	FSK
Data Transmission Rate (Kbps)	0.3	10	8	1.2	5.28
Number of Channels	600	666	1000	180	222

France: A direct-dial car telephone operating at 160 MHz can access the cellular system. Radiom 2000 is also used in France.

Spain: The NMT 450 MHz cellular networks are utilized in Spain.

Austria: A new NMT cellular network called 'Autotelefonnetz C' have been put into service. The Austrian PT&T has allocated 222 duplex channels in ranges 451.3 to 455.7 MHz and 461.3 to 465.7 MHz.

Germany: C-450 cellular system was installed in Germany. Also France and Germany are working on cross-border compatibility in cellular radio system, and have proposed a CD-900 digital system.

Switzerland: The NMT 900 MHz cellular networks were built in 1986.

Turkey: Turkey's cellular system uses a version of NMT networks.

Today, there is no compatibility among the analog cellular system serving European countries. In 1987, they agreed to set up a pan European digital cellular standard, called GSM (Special Mobile Group) specification. CEPT (Conference Europeenne des Postes et Telecommunications) has made available two frequency bands to be used by the GSM system, namely:

890-915 Mhz for the direction mobile terminal to base station, and

935-960 MHz for the direction base station to mobile terminal.

The GSM modulation is Gaussian Minimum Shift Keying (GMSK). The GSM multiple access technique is a combination of frequency division with carriers spaced at 200 KHz intervals and time division with 8 logical channels per carrier. The data rate is 270.833 Kbps.

Cellular Systems in the United States:

While European and Japanese standards will be applied to completely new systems operating in dedicated frequency bands, the present North American standard specifications are enhanced, rather than replaced. Advanced Mobile Phone System (AMPS) were generated firstly. Then, a digital voice transmission capability was added to new subscriber equipment. The new cellular system is called IS-54. The carrier spacing of both IS-54 and AMPS is 30 KHz and the carrier frequency is 800 MHz. AMPS uses Frequency Shift Keying (FSK) modulation technique, and IS-54 adopts Differential Quaternary Phase Shift Keying (DQPSK) modulation. The data transmission rate for AMPS is 10 Kbps. Like GSM, IS-54 has data rate 48.6 Kbps.

QUALCOMM is developing a system with digital transmission based on spread spectrum Code Division Multiple Access (CDMA). It is optimized for service (voice quality, voice activity, handoff) and environment (time varying fading, radial attenuation, etc.,). It has high capacity which is achieved by instantaneous optimal

utilization of all constituents: Frequency, time, space and activity. It also applies multidimensional diversity. The spread spectrum bandwidth is set at 1.25 MHz in 800 MHz and transmission rate is 9.6 Kbps. Quadrature Phase Shift Keying (QPSK) is used in spread spectrum modulation. The system will operate in existing bands.

Cellular Systems in the rest of the world:

Australia is installing a system using Ericsson's AXE-10 switching network and will operate at 800 MHz.

Kuwait's cellular system uses NEC's switches, which operates at 800 MHz.

Hong Kong has three systems. The United Kingdom's TACS system, the United States' AMPS system, and Japanese NEC system were installed in Hong Kong.

2.3 Multiple Access Techniques

The basic aim of present day mobile communication systems is to maximize the capacity in terms of the number of users. This has resulted in a concentrated effort to develop more spectrum efficient modulation. Thus, multiple access communication techniques have been brought about.

In multiple access communications, users share the available channel bandwidth. This means that the overall channel is divided into sub-channels and then assigned to mobile radios. There are a number of techniques for multiple access schemes. In narrowband cellular systems, Frequency Division Multiple Access (FDMA) and Time Division Multiple Access (TDMA) are employed. However, in wideband cellular systems, Code Division Multiple Access (CDMA) can be used.

In the following subsections, multiple access techniques will be explained briefly.

2.3.1 Frequency Division Multiple Access (FDMA)

It is the simplest way to divide up the total radio channel capacity. FDMA splits the frequency band into disjoint sub-bands and two radios can communicate using a sub-band or frequency. There would be no interference between radio signals whose spectra occupy disjoint parts of the total available frequency band [22].

2.3.2 Time Division Multiple Access (TDMA)

TDMA is another way of increasing spectrum channel efficiency. It has also the potential to reduce the cost of both cell size and mobile terminal equipment. Here, time is divided into disjoint slots where any two mobile radios communicate using assigned time slots. For example, in GSM system the spectrum space is segmented in time which has time slots with length 0.577 ms. Eight slots numbered 0 to 7 form a time frame with length 4.615 ms. One user is designated in one time slot every 4.615 ms. This structure is applied in both uplink and downlink directions [25].

In principle, TDMA and FDMA are equal in spectral efficiency. However, in practice TDMA is more flexible than FDMA because time slots can be easily changed without requiring hardware changes in the system. Besides, a radio can receive data from many other radios with only one receiver since their transmission time slots do not overlap. However, in a heavy traffic area, TDMA performance may degrade faster than FDMA performance.

2.3.3 Code Division Multiple Access

CDMA is a multiple access scheme that has been used for many years in military communications. Since CDMA increases capacity and improves quality, it has been applied to cellular mobile communication.

In CDMA spread spectrum systems, data signal is spread by using a unique pseudorandom (PN) signal before transmission. Since each user has an individual spreading code, a large number of CDMA signals can be transmitted in the same spectrum. At the receiver, the received signal is despread by using the pseudorandom (PN) sequence synchronized with the user's spreading signal. A more detailed discussion on CDMA will be given in Chapter 3.

CHAPTER III

SPREAD SPECTRUM SYSTEMS

3.1 Introduction

Spread spectrum is a means of transmission which has a bandwidth much greater than the minimum bandwidth required to transmit the digital information. The spreading of the spectrum is accomplished by using a wideband encoding signal.

There are two basic elements in the design of spread spectrum systems. The bandwidth expansion is much greater than unity, i.e, the transmitted signal must occupy a bandwidth which is much larger than the information bit rate. Spreading can mitigate the severe effects of interference, such as multipath reception in urban mobile radio communications. Since coded signals are characterized by a bandwidth expansion factor, coding is an important element in spread spectrum systems. The model for spread spectrum systems is shown in Fig. 3.1.

A second element is the spreading sequence, which is pseudorandom (PN), i.e, the signal is similar to random noise and difficult to demodulate by receivers other than the desired one.

The same spreading signal is used in the receiver operating in synchronism with the transmitter to despread the received signal so that the original data can be recovered.

Spread spectrum systems have been applied primarily in military communications. However, their importance increases day by day in civil applications

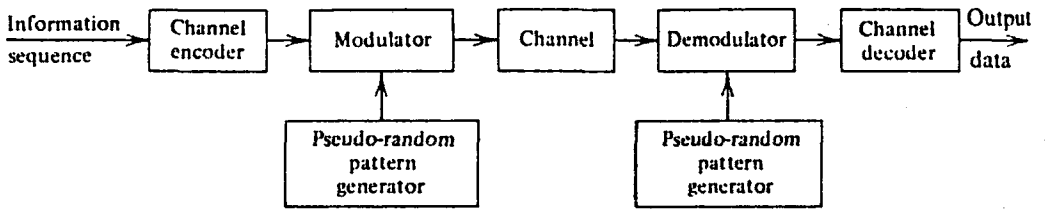

Figure 3.1. Model of Spread Spectrum Systems

as well. In addition to communications, they are applied in radar and navigation to obtain accurate range (time delay) and range rate (velocity) measurements [9].

In this work, only the application of spread spectrum systems in communications will be considered.

There are certain features that make spread spectrum systems attractive[9]. They have the advantages of :

1. combatting the deleterious effects of interferences, i.e, interference due to jamming, multipath propagation, and other users of the channel,

2. hiding a signal that is transmitted at a low power, i.e, it has low detectability property,

3. achieving message privacy,

4. code division multiplexing .

There are several basic techniques to spread a signal. One method of spreading the spectrum of a data signal is to modulate the signal using a very wideband signal. Since the spreading signal has a bandwidth much larger than the data bandwidth, the transmission is dominated by the spreading signal. Bandwidth spreading by a wideband signal is called Direct Sequence (DS) spread spectrum. The block diagram is shown in Fig. 3.2.

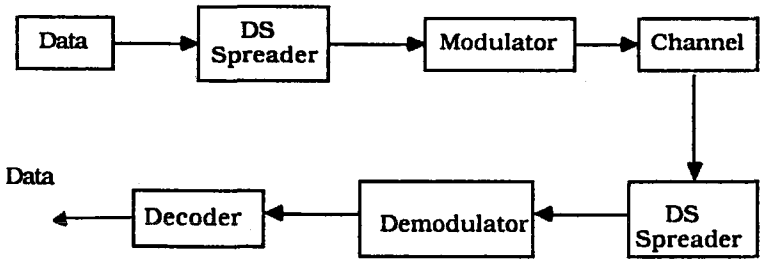

Figure 3.2. Block Diagram of DS Spread Spectrum Systems

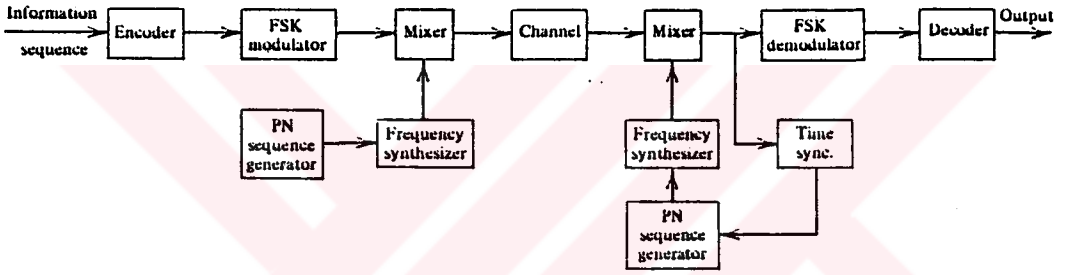

Figure 3.3. Block Diagram of FH Spread Spectrum Systems

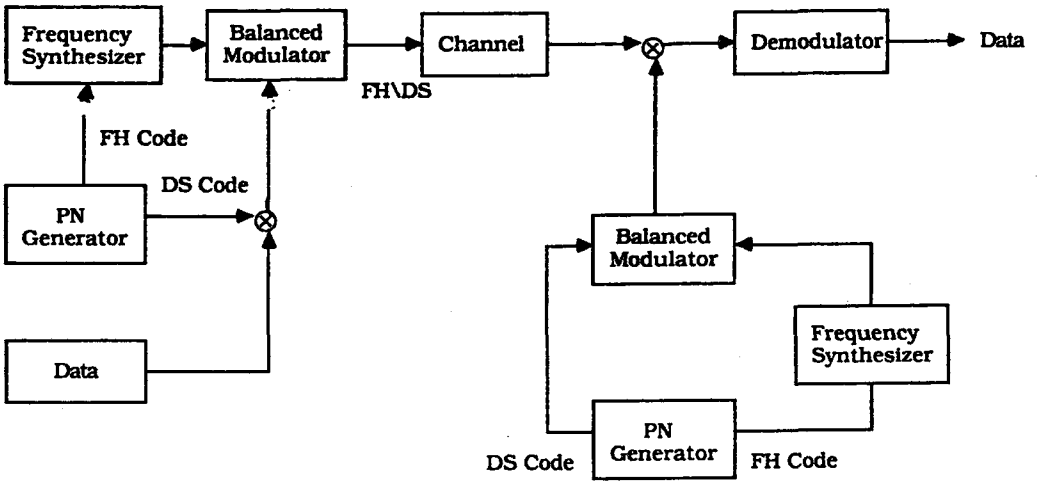

Figure 3.4. Block Diagram of FH / DS Spread Spectrum Systems

A second method for widening the spectrum of a data modulated carrier is to change the carrier frequency in a pseudorandom (PN) manner. Since a data modulated carrier hops from one frequency to the next, this type of spread spectrum is called Frequency Hopping (FH) spread spectrum. In the receiver, there is an identical pseudorandom generator and the frequency hopping is removed by mixing with a local oscillator signal that is hopping synchronously with the received signal. Fig. 3.3 illustrates a typical FH spread spectrum.

A third method for spectrum spreading is to employ both direct sequence and frequency hopping spreading techniques in a hybrid form (Frequency Hopping/Direct Sequence, FH/DS), which offers certain advantages over the direct sequence and the frequency hopping techniques. The block diagram is shown in Fig. 3.4. Hybrid forms are widely used in military spread spectrum systems and are currently the only practical way of achieving extremely wide spectrum spreading.

One reason for using hybrid techniques is that some advantages of the two spread spectrum systems are combined in a single system. In addition, it provides properties that are not available from a single modulation method. For example, the processing gain that is obtained by employing a single spread spectrum technique is limited by the speed of the electronic components used. However, using the same components, the maximum processing gain can be increased by employing more than one spread spectrum modulation technique in a combined form.

In this work, only direct sequence spreading is considered.

3.2 Direct Sequence Spread Spectrum

Direct sequence spread spectrum systems are the best known and the most widely used spread spectrum systems [9,18].

Direct sequence spread spectrum, as the name implies, is accomplished by spreading bandwidth of a data modulated carrier directly by using wideband binary signals. The spreading signal has some properties that facilitate the demodulation of the transmitted signal by the intended receiver, and that render demodulation as

difficult as possible to an unintended receiver. The bandwidth of the spreading signal is larger than the data bandwidth, therefore the spread spectrum signal has a bandwidth dominated by the spreading signal.

There are various techniques used for direct sequence spreading [18]:

(1) Binary Phase Shift Keying (BPSK) Direct Sequence Spreading,

(2) Quadrature Phase Shift Keying (QPSK) Direct Sequence Spreading,

(3) Minimum Shift Keying (MSK) Direct Sequence Spreading .

The most common forms of direct sequence spread spectrum used in practice are BPSK and QPSK direct sequence spread spectrum.BPSK is the simplest form of direct sequence spread spectrum. It is sometimes advantageous to transmit the signal simultaneously on two quadrature carriers. The same bit error probability is achieved by using half of the transmission bandwidth. However, bandwidth efficiency is not usually important for spread spectrum systems. Quadrature modulations are less sensitive to some types of jamming and more difficult to detect in low probability of detection applications [18].

In the following section, BPSK direct sequence spread spectrum systems will be investigated.

3.3 BPSK Direct Sequence Spread Spectrum

The most common form of direct sequence spread spectrum is BPSK of a carrier by a binary sequence. Generally, the same type of modulation is used for both the data and the spreading signal. When BPSK modulation is applied, one phase modulator can be eliminated.

Ideally, BPSK modulation results in the phase change of the carrier by 180 degrees. In BPSK direct sequence spread systems, the phase of the carrier is shifted pseudorandomly (180 degrees).

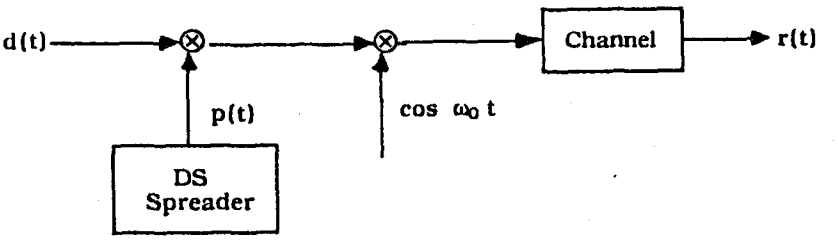

Figure 3.5. Block Diagram of BPSK DS Modulator

It can be represented mathematically as a multiplication of the data modulator carrier by a function that takes on the values (±1).

Typically, the direct sequence biphase modulator has the form shown in Fig. 3.5 where d(t) is a (±1) binary data signal and p(t) is a (±1) binary spreading signal. The spreading is represented by the multiplication of d(t) with p(t). The resultant signal is given by

$$s(t) = d(t)p(t)\cos(w_0 t) \qquad (3.3.1)$$

where w_0 is a carrier frequency.

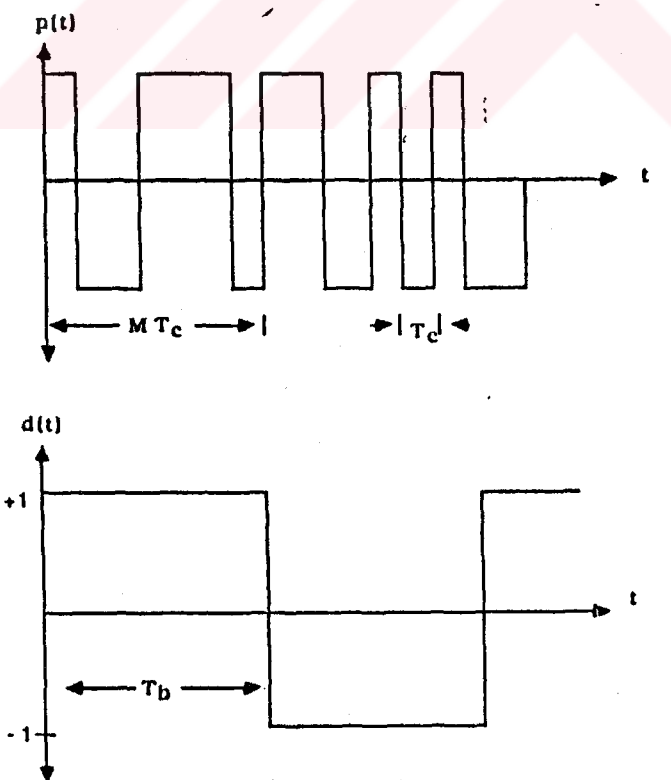

Figure 3.6. Data and Spreading Signal

Fig. 3.6 illustrates the data signal and the spreading signal p(t). We assume that the information rate is R bits/sec , and that the available channel bandwidth is W Hz. In order to utilize the available channel bandwidth, the phase of the carrier is shifted pseudorandomly by using a pseudorandom generator at a rate W times/sec. The duration corresponding to the pseudorandom sequence (or spreading sequence) is called the chip duration T_c, which is the reciprocal of W. Similarly, the reciprocal of R, denoted as T_b, defines the duration of rectangular pulse corresponding to the transmission time of a data signal and its time duration T_b is called the bit interval.

The bandwidth expansion factor can be defined in terms of the data rate and the spreading signal rate:

$$B_c = W / R \tag{3.3.2}$$

or equivalently

$$B_c = T_b / T_c \tag{3.3.3}$$

In practical systems, T_b / T_c is a positive integer,

$$M = T_b / T_c \tag{3.3.4}$$

where M is called the number of chips per bit duration.

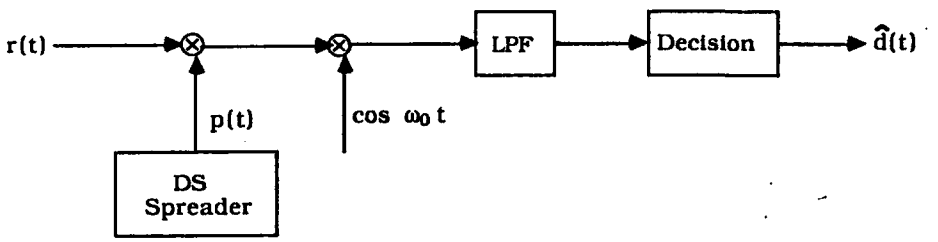

Figure 3.7. Block Diagram of BPSK DS Receiver

In Fig. 3.7 the simplified block diagram of BPSK direct sequence spread spectrum receiver is shown. At the receiver side, the received signal is multiplied by the spreading signal to despread it. It is assumed that the spreading signals of both transmitter and receiver are the same and synchronized with each other. Then, the despread signal is multiplied with the carrier to transform the signal to its baseband equivalent. Any incoming signal, which is not synchronous with the spreading signal and the carrier frequency, is spread to a bandwidth of the spreading signal. Therefore, the lowpass filter (LPF) is used to reject the undesired signals. Then, the filtered signal is input to the decision circuit, where the data signal d(t) is estimated.

3.4 CDMA Channel Capacity

The maximum number of simultaneous users that could be accommodated at a specific bit error rate is of interest in analysing a digital mobile radio system.

We will investigate the number of users in the consideration of a power control because we assume that all signals in the channel, including the desired one, arrive at a receiver at the same power level.

In the following subsections, the capacity will be simply derived for both the single cell and multicell cases.

3.4.1 Single Cell

The transmission of a single bit is considered. The received bit power from any mobile is P, and therefore, the received bit energy E_b can be expressed as

$$E_b = P * T_b \qquad (3.4.1.1)$$

where T_b is the bit duration, and γ is the required signal_to_noise ratio (SNR) to achieve a specified bit error probability P_b,

$$\gamma = E_b / N_o \qquad (3.4.1.2)$$

where N_o is the noise spectral density.

It is assumed that the number of users in a cell is given as N. We also consider one user and the sum of the influences from all other users' interference in the same cell.

With the transmission bandwidth W, the received power P per user, the number N of users, and the additive white Gaussian noise spectral power density N_o', the spectral power density N_o of the noise in the receiver is given by

$$N_o = (P/W) * (N-1) + N_o' \qquad (3.4.1.3)$$

Using Eq. 3.4.1.2 and Eq. 3.4.1.3, γ is approximately equal to

$$\gamma = W*T_b / N \qquad (3.4.1.4)$$

From Eq. 3.4.1.4, it can be seen that the number of users N is

$$N = W*T_b / (E_b / N_o) \qquad (3.4.1.5)$$

Since T_b is the reciprocal of the bit rate,

$$N = (W/R) / (E_b / N_o) \qquad (3.4.1.6)$$

and W/R is defined as M in section 3.3, finally, N becomes

$$N = M / (E_b / N_o) \qquad (3.4.1.7)$$

3.4.2 Multicell

As mentioned before in Chapter 2, frequency reuse is the essential feature of cellular mobile communication systems. In CDMA, frequency reuse efficiency is determined by the SNR resulting from all the system users within the range, not just those in any given cell site. Table 3.1 shows frequency reuse factors for different systems.

Table 3.1 Frequency Reuse Factors In Different Systems

QUALCOMM - CDMA	Between 3/5 and 1
GSM - TDMA	1/4 or 1/3
NA -TDMA (IS - 54)	1/7
AMPS	1/7

Considering the frequency reuse scheme, the number of users in Eq. 3.4.1.7 becomes

$$N = M * f_u / (E_b / N_o) \qquad (3.4.2.1)$$

where f_u is the frequency reuse efficiency.

Any interference present in the wideband channel, including that of other CDMA users can be suppressed by exploiting the voice activity that allows users to obtain multiple access to the same spectrum, including those in adjacent cells. On transmission, first the speech signal is vocoded. The vocoder also detects the silence periods in natural speech flow and this signal is used to gate the CDMA transmitter on or off. By exploiting the voice activity factor (typically, 50% of time the speaker is quiet), the mutual interference between CDMA users can be drastically decreased. Thus the spectral efficiency of the network increases.

Considering the voice activity, CDMA capacity Eq. 3.4.2.1 becomes

$$N = M * f_u * (1/d) / (E_b / N_o) \qquad (3.4.2.2)$$

where d is the effective voice duty cycle.

In certain locations and special situations, the sector angle can be narrowed in order to assign more channels in one sector without increasing the neighbouring channel interference. This process is called sectorization. There are various types of sectorized cells such as the 120 degrees_sector cell, the 60 degrees_sector cell, the 45 degrees_sector cell. Narrowing the sector reduces the total interference of users in the sector to increase the capacity proportionally. This means that the capacity of CDMA is enhanced. Finally, the capacity formula is

$$N = M * f_u * (1/d) * S / (E_b / N_o) \qquad (3.4.2.3)$$

where S is the number of sectors in a cell.

3.5 Advantages and Disadvantages of CDMA Spread Spectrum Systems

3.5.1 Advantages of Spread Spectrum Systems

The CDMA spread spectrum systems have some properties to overcome the severe problems of mobile communications such as fading, multipath and capacity.

In this sub-section we will try to set forth the advantages of CDMA techniques over FDMA and TDMA systems.

3.5.1.1. Spectral Efficiency

Since the number of users could vary depending on the available bandwidth or on the information bit rate, a measure defined as spectral efficiency is also useful :

$$\eta = R / (W / N) \qquad (3.5.1.1.1)$$

where η is spectrum efficiency, N is the number of users simultaneously served by the system, R is the bit rate per user, and W is the transmission bandwidth. We note that η is defined as the bit rate divided by the bandwidth per user.

Using Eq. 3.4.1.7 , we can see that the spectral efficiency of a single CDMA cell is inversely proportional to E_b/N_o and Eq. 3.5.1.1.1 becomes

$$\eta = 1 /(E_b / N_o) \qquad (3.5.1.1.2)$$

For the multicell network, using Eq. 3.5.1.1.2 the spectral efficiency becomes

$$\eta = f_u * (1/d) * S / (E_b / N_o) \qquad (3.5.1.1.3)$$

The capacity (bits/sec/Hz/user/cell) comparison of different systems are given in Table 3.2.

Table 3.2 Capacity Comparison for Different Systems

	bits/sec/Hz/user/cell	bandwith/user (KHz)
AMPS	1/21	210
NA - TDMA	1/7	70
GSM - TDMA	1/10 or 1/7.5	100 or 75
QUALCOMM - CDMA	9/10	10.67

With TDMA and FDMA, the maximum number of users is an exact quantity. When the number of users reaches the maximum value, no additional users can be handled. However, in CDMA systems, there is no exact limit on the number of users. If the number of active users increases, the quality degrades continuously for all users. This feature is known as soft degradation, which is typical for CDMA spread spectrum systems [14].

3.5.1.2 Diversity Gain In Multiple Environment

a) Frequency Diversity

We are interested in frequency selective channel where channel bandwidth is much greater than the coherence bandwidth of the channel. Since, with FDMA, each user has a limited frequency band, FDMA has no diversity by distributing the symbol energy along the frequency axis. However, TDMA and CDMA have perfect frequency diversity, because they spread the symbol energy over the entire channel.

b) Path Diversity

The path diversity is another capability of CDMA spread spectrum systems. The pseudorandom sequence(PN) has essentially zero correlation for time offsets greater than one chip time. Thus, when the difference in path delays for the various paths exceeds the PN chip duration, the wide bandwidth PN allows different propagation paths to be separated.

A transmitted signal having bandwidth much greater than the coherence bandwidth of the channel is utilized to provide the receiver with several independently fading signal paths. RAKE receiver, invented by Price and Green (1958), resolves

these signals, and hence, profits from the diversity. In other words, RAKE receiver 'collects' the energy from the various transmission paths. Then, resolved signals are used in a diversity combining scheme in order to maximize the total desired signal-to-noise energy at the input of the demodulator.

Optimum diversity combining can be achieved if a Maximal Ratio Combining (MRC) technique is implemented in the form of a RAKE receiver. In the MRC process, signals (paths) are weighted proportionally to their individual signal voltage_to_noise power ratios (their path attenuations) and then summed. However, this process requires that the amplitude and phase of every diversity path are estimated continuously. If accurate amplitude and phase estimation cannot be accomplished, equal gain combining (EGC) may yield a better performance.

By using a RAKE receiver with MRC scheme, an important loss in performance occurs only if all paths fade at the same time, as when a path suffers from a fast fading which cannot be tracked, there are other paths still to be processed by the RAKE receiver.

3.5.1.3 Interleaving and Forward Error Correction (FEC)

Even though spread spectrum techniques are used to overcome multipath fading and thus provide a reliable and high quality channel, the spectral efficiency of the system can be poor. In order to combat the effects of fading, Forward Error Correction (FEC) coding can be employed with a relatively small increase in data rate. Thus, the spectral efficiency of the system can be enhanced. FEC coding reduces the BER of the uncoded channel by adding redundancy to the coded data signal. This can be implemented using different techniques such as block, convolutional and trellis codes. In CDMA spread spectrum systems optimum performance is obtained if the channel errors seen by the FEC scheme are independent (uncorrelated) of each other. Since errors often occur in bursts, it is necessary to interleave the FEC data to get uncorrelated errors in consecutive data bits. Hence, time diversity is obtained.

Due to deep fading in FDMA, burst errors occur more frequently. TDMA, because of burst transmission, is vulnerable to short time impulsive noise. However,

continuous transmission is used in CDMA. Hence, FEC and interleaving are not a problem as in TDMA and FDMA.

3.5.1.4 Soft Handoff and Cell Diversity

In the CDMA cellular system, the same frequency is used in all cells. When a mobile unit enters the new cell's coverage area, the mobile unit detects the pilot channel of the new cell and reports it to the original cell. The new cell assigns a modulator_demodulator (modem) unit to the call while the old cell continues to handle the call. Thus, handoff process is initiated. The cell site modem searches for and finds the mobile's signal. It also begins transmitting the outbound signal to the mobile, for which, the mobile unit searches . When the mobile unit finds the new cell site signal, it starts to listen to it. The mobile sends a control message to indicate that the handoff process is complete. This type of operation is known as 'make before break'.

The Soft Handoff process provides the cell diversity. In this diversity mode, the process is initiated as explained before. The mobile unit determines that a neighbouring cell site has a signal strength high enough to allow good quality demodulation. Then, it transmits a control message to the cell site and requests the cell diversity mode. The system controller responds by connecting the call to the new cell site modem. It also performs diversity combining of the signals received by the two cell sites (on a vocoder frame by vocoder frame basis). Likewise, the mobile unit combines the transmitted signals from the cell sites. The cell site diversity mode is terminated when the mobile unit determines that only one cell site is providing adequate signals for quality reception.

3.5.2 Disadvantages of Spread Spectrum Systems

There have been mainly two problems in CDMA spread spectrum systems. One of them is the system complexity and the need of high speed electronic equipment because of using wideband spectrum. However, as microelectronics technology develops rapidly, it makes very complicated digital signal processing

feasible. The second problem is the necessity of power control. In this section, only power control is discussed.

Power Control:

Without power control of each transmitter,near/far, fading and shadowing effects make CDMA spread spectrum systems almost useless.

In mobile communications, random geographic distributions of transmitters, multipath and fading causes the reception of the signals to be at different power levels. In addition, the cell site receivers are captured by a single user who may be near the base station, and thus prevent any distant users from communicating. This is commonly known as the 'near/far' problem. In order to provide reliable communications, power control must be employed.

Considering QUALCOMM's system, we see that power control is used both on uplink (mobile→base) and on downlink (base→mobile). In the near/far problem, mobile stations near the cell base station have a smaller path loss and thus create more interference that significantly reduces the capacity. In order to solve this problem, the CDMA system uses two types power control on uplink : open loop and closed loop.

In open loop power control, the mobile station adjusts its transmitted power using the total received power in the receiver. The open loop power mechanism is very fast and is especially effective in quickly controlling the mobile station's transmitted power. This is useful when emerging from a shadow, such as from behind a large building.

In open loop power control, each mobile unit estimates the path loss from the cell site to the mobile unit. The stronger the received signal, the lower will be the mobile's transmitted power. Reception of a strong signal from the cell site indicates that the mobile is either close to the cell site or has an unusually good path to the cell site. This means that relatively less mobile transmitter power is needed. The open loop

power mechanism adjusts the mobile transmit level quickly downward, preventing the mobile transmitter power being at too high a level.

When the received signal is weak, the mobile's transmitter power is increased. However, the rate of increase of mobile transmit power is limited by the closed loop power mechanism because if the channel for one mobile suddenly improves, then the signal received at the cell site from this mobile will increase in power, causing additional interference to all the other signals sharing the same wideband channel.

In addition to measuring the received signal strength in the mobile, the cell site's transmit power and antenna characteristics and the number of active calls are also required. This allows the mobile's microprocessor to compute the reference power level. Besides, it allows the system to have cell sites with differing transmit power levels and antenna gains (ERP levels) corresponding to the size of the cells.

The second type of power control is closed loop method. The cell compares the received power from the mobile station to a desired signal power and warns the mobile unit to decrease or increase its transmitted power. The closed loop power control counteracts errors from the open loop power control process. If the mobile station were only receiving a single cell and if the mobile station knew the total ERP of the cell, then it could effectively determine the path loss and know the correct transmit power to get a particular received E_b/N_0 at the cell. Since the total ERP of the cell is not known exactly and since the received power may have contributions from various cells, closed loop power control sets the gain between the received AGC (Automatic Gain Control) level and the transmitted power. Although the cell transmit power is known, the path loss on downlink CDMA Channel may differ from that on uplink CDMA Channel.Thus the mobile unit cannot determine the required transmit power correctly. Closed loop power control also solves this problem.

On downlink, the mobile station measures the received signal quality. Then, it sends the results of this measurement to the cell. If the quality is poor (i.e., less than a desired minimum value), the cell evaluates the power needs of all the mobiles using the cell and decides whether to increase the code channel power to that mobile station. The cell can either increase its total transmit power, which is disadvantageous to mobile stations using other cells due to increasing interference, or

the cell can redistribute power from mobile stations with good quality to the disadvantaged mobile station.

CHAPTER IV

CHANNEL MODEL

4.1 Introduction

This chapter presents a summary of the channel model used in simulation [1,3]. The statistical channel model is based on experimental data. This model characterises the urban radio propagation medium in various urban environments. The measurements were carried out at three frequencies (488, 1280, and 2920 MHz) and at four areas around San Francisco Bay area. In this study,the experimental data, at 1280 MHz and at a medium size city (Downtown of Oakland) are used. The spatial resolution used in the simulation is 3 feet.

In mobile communications, after transmitting a pulse, a sequence of pulses is received due to reflections, refractions and scattering. It is known as multipath fading. The signals arriving from indirect paths and the direct path (if it exists) combine and distort the transmitted signal. In continuous wave (CW) transmission, the multipath medium causes fluctuations in the received signal amplitude. In pulse transmission, on the other hand, the effect of multipath is to produce a series of echo pulses for each transmitted pulse [1,2].

Each multipath component has random amplitude, propagation delay and phase shift due to movement of the mobile unit and obstacles. The channel is modeled as a tapped delay line filter [7]. The impulse response is given by

$$h(t) = \sum_{k=0}^{\infty} a_k \, e^{j\theta_k} \, \delta(t-t_k) \qquad (4.1.1)$$

where $\{t_k\}$ is a set of arrival times, $\{a_k\}$ is a set of amplitudes, and $\{\theta_k\}$ is a set of phases. A graph illustrating h(t) is shown in Fig. 4.1.

This plot has 7 profiles separated by a 3 feet spatial sampling distance. The delay spread is taken to be 76 bins that correspond to an excess delay of about 7 microseconds. It is noticed that the paths beyond 3.5 microseconds are usually the weak paths.

4.2 Simulation of Arrival Times

In urban propagation, since the obstacles are randomly located in space, the arrival times are random variables. In Hashemi's simulation program (called SURP), the set of arrival times is generated according to a modified Poisson process suggested by Turin, i.e., the path arrivals follow a Poisson distribution with a mean arrival rate that jumps whenever a path arrives. This model is a branching process [1].

The time axis, which has its origin at the line-of-sight (LOS) path delay, is divided into 100 nsec intervals (bins). In every bin, it is checked whether a path is present or not. If a path occurs, it increases the probability of having a path in the next interval by a factor K, which was found by the empirical data by Suzuki [3]. In this model, the probability of having more than one path in the same interval is assumed to be zero due to bandwidth limitations of the receiver. If two or more paths have delays less than 100 nsec, they are combined and considered as a single path.

For the first profile, the probability of having a path in a bin i, P is given by

$$\begin{aligned} P_i &= \lambda_i && \text{if there is no path in the } (i\text{-}1)^{st} \text{ bin,} \\ P_i &= K\lambda_i && \text{if there is a path in the } (i\text{-}1)^{st} \text{ bin.} \end{aligned} \qquad (4.2.1)$$

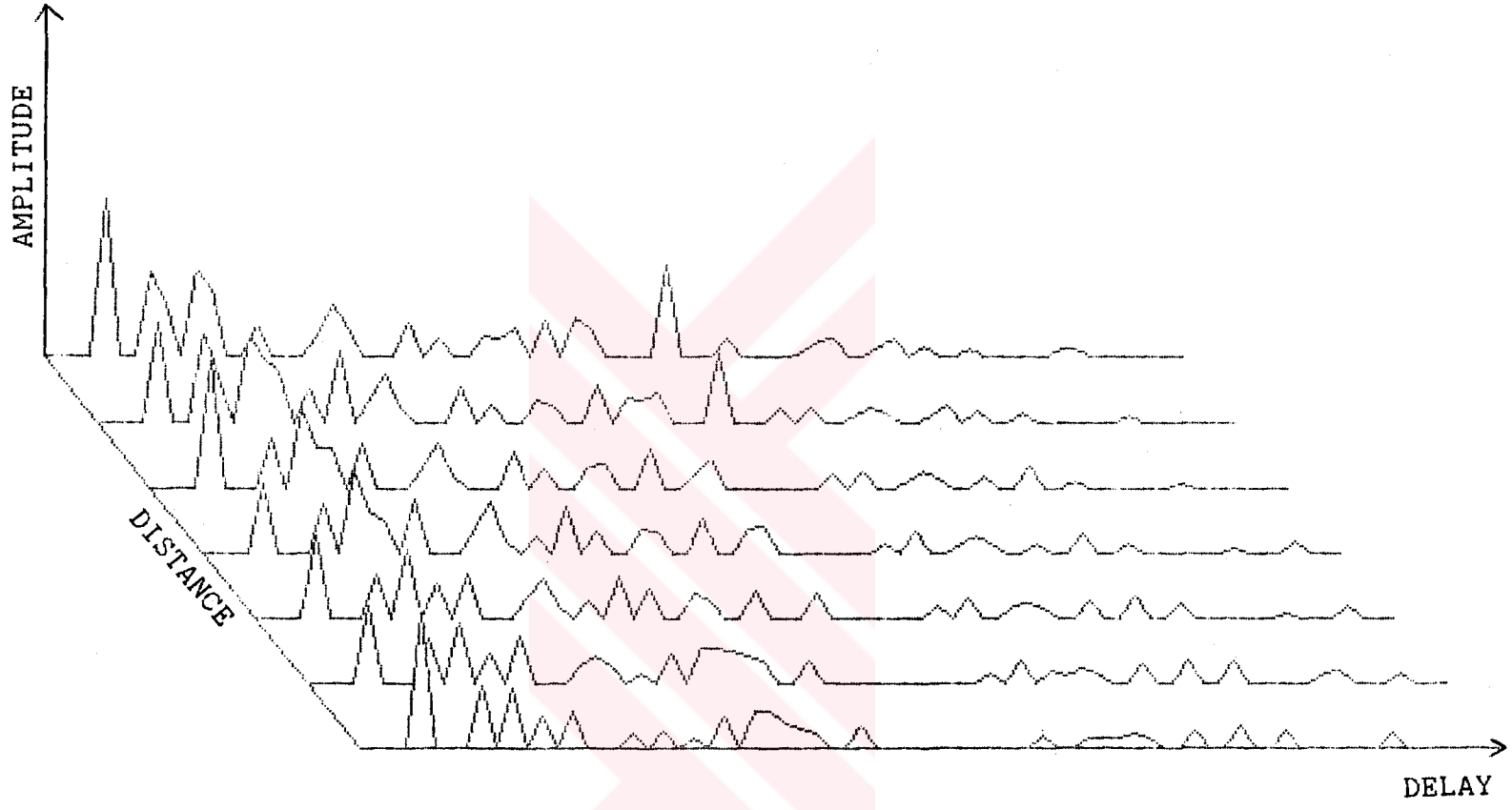

Figure 4.1. Impulse Responses of the Channel

The path probability λ_i is found from the equations:

$$\lambda_1 = r_1$$

(4.2.2)

$$\lambda_i = \frac{r_i}{(K-1)r_{i-1}+1}, \quad (i \neq 1)$$

where r_i is the empirical probability of occurrence.

For the other profiles, spatial correlations i.e., correlations on adjacent profiles) are taken into account. The probability of having a path P_i is modified to:

$P_i = \alpha(d)\lambda_i$ if there is a path in the i^{th} bin of the previous profile and no path in the $(i-1)^{st}$ bin of the profile. (4.2.3.a)

$P_i = \alpha(d)K\lambda_i$ if there is a path in the i^{th} bin of the profile and a path in the $(i-1)^{st}$ bin of the profile. (4.2.3.b)

$1-P_i = \beta(d)(1-\lambda_i)$ if there is no path in the i^{th} bin of the previous profile and no path in the $(i-1)^{st}$ bin of the profile. (4.2.3.c)

$1-P_i = \beta(d)(1-K\lambda_i)$ if there is no path in the i^{th} bin of the previous profile and a path in the $(i-1)^{st}$ bin of the profile. (4.2.3.d)

where d is the distance between samples, $\alpha(d)$ and $\beta(d)$ are decreasing functions to control the correlations.

Finally, the path arrival sequences of 0's and 1's, which show the absence or presence of a path, are generated according to the above process.

4.3 Simulation of Amplitudes

In this model, all amplitudes are generated according to the lognormal distribution given by

$$p(a) = \frac{1}{\sqrt{2\pi\sigma}a} \exp\left(\frac{[\ln(a)-\mu]^2}{2\sigma^2}\right) \qquad a \geq 0 \qquad (4.3.1)$$

In the simulation of the amplitudes, correlations are taken into account:

a) Temporal_Correlation : It is a correlation in time, i.e., the adjacent paths of the same profile are correlated due to reflection, refraction, and scattering by the same structure.

b) Spatial_Correlation : It is a correlation in space, i.e., the paths of adjacent profiles , whose arrival times are about the same, are correlated. Because a mobile moves by a small distance, the reflectors and scatters are almost the same.

Since the urban channel is not statistically homogeneous, the mean and the variance of the amplitudes are also random. The log-mean and the log-variance are spatially correlated and generated according to the bivariate normal distributions.

The amplitudes are generated in dB in the following way: For the first profile, the means and the variances are generated according to the lognormal distribution by using parameters estimated from empirical data. Then the first path amplitude is generated according to the normal distribution. For the other path amplitudes, temporal correlations are considered. They are generated according to the conditional normal distributions. The condition is the closest path in the same profile, and the temporal correlation is a decreasing function of the difference in arrival times of the two paths. The temporal correlation is given by

$$\rho = \exp\left(-\frac{\delta}{(\tau_t)_i}\right) \qquad (4.3.2)$$

where δ is the difference between the arrival times of two adjacent paths, and $(\tau_t)_i$ was obtained by starting with a reasonable value and changing it repeatedly (in the simulation program) until desirable temporal correlation coefficients were obtained by matching experimental and simulational distributions.

For the other profiles the means and variances are generated according to the lognormal distributions if there is no path in the same interval of the previous profile. Otherwise, the conditional lognormal distributions are taken into account.

After generating the means and variances, the amplitudes are generated as follows: For the first path, only the spatial correlation with the previous profile is considered. For the other paths, both the spatial and the temporal correlations are taken into account. Then, the amplitudes are generated according to the conditional normal distribution. This is illustrated in Fig. 4.2.

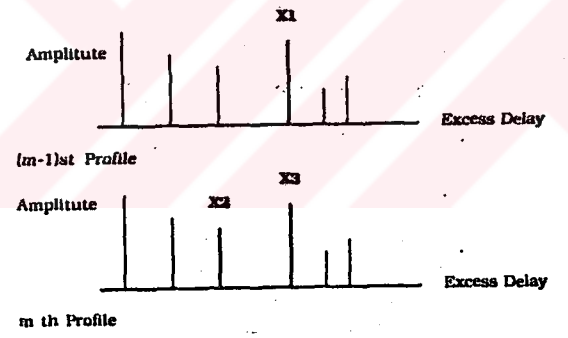

Figure 4.2. Two Consecutive Samples of the Channel's Impulse Response

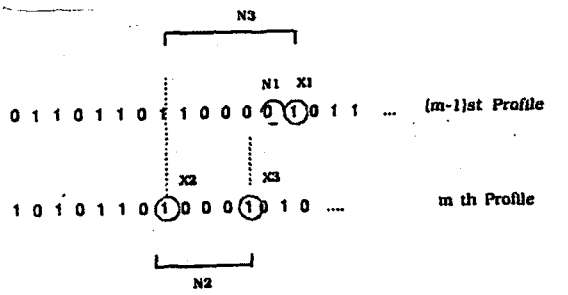

Figure 4.3. Two Consecutive Sequences of Arrival Times Illustrating N_1, N_2, N_3

Let X_2 and X_3 be the log_amplitudes of the $(j-1)^{st}$ and j^{th} path of m^{th} profile respectively (j=2,3,4,..,m=2,3,4,....), and X_1 represents the log_amplitude of the path in the $(m-1)^{st}$ profile whose arrival time is closest to that of X_3. A three dimensional normal distribution for X_1, X_2, X_3 is assumed to take into account both spatial correlation (i.e., correlation between X_2 or X_3 and X_1), and temporal correlation (i.e., correlation between X_3 and X_2). In the simulation, X_3 is generated according to a conditional normal distribution with the conditions being X_1 and X_2, i.e., X_3 has a normal distribution with mean μ and variance σ^2 given by

$$\mu = \mu_3 + \frac{(\rho_{13}-\rho_{12}\rho_{23})}{1-\rho_{12}^2}\frac{\sigma_3}{\sigma_1}(x_1-\mu_1) + \frac{(\rho_{23}-\rho_{12}\rho_{13})}{1-\rho_{12}^2}\frac{\sigma_3}{\sigma_2}(x_2-\mu_2) \tag{4.3.3}$$

and

$$\sigma^2 = \frac{\sigma_3^2}{1-\rho_{12}^2}\left(1 - \rho_{13}^2 - \rho_{23}^2 - \rho_{12}^2 + 2\rho_{12}\rho_{13}\rho_{23}\right) \tag{4.3.4}$$

where $\mu_i = E\{Xi\}$, $\sigma^2_i = var\{X_i\}$, i = 1,2,3 and ρ_{ij} (i=1,2,3:j=1,2,3, $i \neq j$) is the correlation coefficient between X_i and X_j.

The method used to evaluate ρ_{12} , ρ_{23} , ρ_{13} can be illustrated with the help of Fig. 4.3, which shows two consecutive sequences of 1's and 0's that represent the presence or the absence of a path. The correlation coefficients are taken to be of the form

$$\rho_{13} = (\rho_s)_i \exp\left\{\left(\frac{-100\,(N_1+1)}{(\tau_t)_i}\right)\right\} \tag{4.3.5}$$

$$\rho_{23} = \exp\left\{\left(\frac{-100\,(N_2+1)}{(\tau_t)_i}\right)\right\} \tag{4.3.6}$$

$$\rho_{12} = (\rho_s)_i \exp\left\{\left(\frac{-100\,(N_3+1)}{(\tau_t)_i}\right)\right\} \tag{4.3.7}$$

where

N_1 : number of 0's between the i^{th} bin of the $(m-1)^{st}$ profile and the closest bin to the i^{th} in the $(m-1)^{st}$ profile that has a 1,

N_2 : number of 0's between the 1 corresponding to X_2 and the 1 corresponding to X_3,

N_3 : difference between the bin number for the amplitude X_2 and the bin number corresponding to X_1,

$(\rho_s)_i$ is the spatial correlation coefficient for the i^{th} bin, estimated from Suzuki's data reduction [3], and parameter $(\tau_{t)_i}$ is the same as that in Eq. 4.3.2.

This procedure continues until the last path amplitude of the last profile is generated.

4.4 Simulation of Phases

In the simulation, the phase sequence $\{\theta_k\}$ are generated for every profile. The phase of a path is assumed to be uniform $[0,2\pi)$. Neither the spatial nor temporal correlations are taken into account. This is valid when the sampling distance is not too small. If the sampling distance exceeds (1/4) to (1/2) of a wavelength, the spatial correlation on the phases is approximately zero. This has also been shown experimentally by Nielson[31]. However, if the distance between samples is very small, this assumption is not correct. In this work, sampling distance is 3 feet, which is sufficient to assume the phases as independent.

CHAPTER V

SYSTEM MODEL AND PERFORMANCE ANALYSIS

5.1 System Description

In this chapter, the simulated system's model depicted in Fig. 5.1 is to be introduced. As mentioned earlier, one method of spreading the spectrum of a data modulated signal is to modulate the signal a second time using a very wideband spreading signal. The BPSK spreading is accomplished by simply multiplying the input binary (±1) sequence $\{d_k\}$ with a pseudorandom (PN) binary sequence $\{p_k\}$. It is assumed that the rate of the spreading sequence is M times greater than that of the data sequence, where M is a positive integer. After spreading the sequence, the resultant signal is input to a pulse shaper which, in turn, drives a product modulator. The BPSK transmitted signal is denoted as:

$$s(t) = \sum_{k=0}^{\infty} d_{[k/M]}\, p_k\, g((t-kT_c))\cos(2\pi f_0 t) \qquad (5.1.1)$$

where

$\{d_k\}$: ±1 ; the data sequence

$\{p_k\}$: ±1 ; binary chips forming the PN sequence

T_c : the chip duration

M : the number of chips in the PN sequence and chips/bit

($T_b = MT_c$ where T_b is the bit duration)

f_0 : the carrier frequency

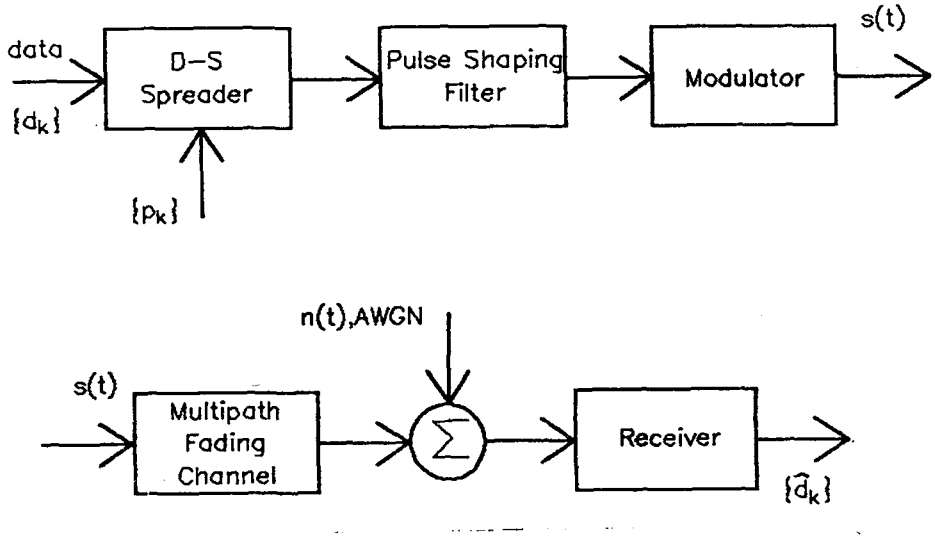

Figure 5.1. Block Diagram of the System

The notation [k/M] refers to the integer part of itsargument. It is assumed that $\{d_k\}$ and $\{p_k\}$ are white, independent sequences composed of equally likely symbols.

The transmitted signal passes through a fading, multipath channel with time-variant impulse response $h(\tau;t)$. The channel can be modeled as a tapped delay line (TDL) with tap spacing T_c and tap coefficients $[a_l e^{j\theta_l}]$. The channel model used in simulation was discussed in Chapter 4 in detail.

The receiver block diagram is illustrated in Fig. 5.2. The received signal is expressed by

$$r(t) = \sum_{l=0}^{L} a_l \left[\sum_{k=-\infty}^{\infty} d_{[k/M]}\, p_k\, g(t-kT_c-lT_c) \cos\left(2\pi f_0 (t-lT_c)+\theta_l\right) \right] + n(t) \qquad (5.1.2)$$

where

a_l : the amplitude of the l^{th} propagation path

θ_l : the phase of the l^{th} propagation path

LT_c : maximum delay spread of the channel

$n(t)$: the white Gaussian noise and interference signal with $N_0/2$ as its power spectral density

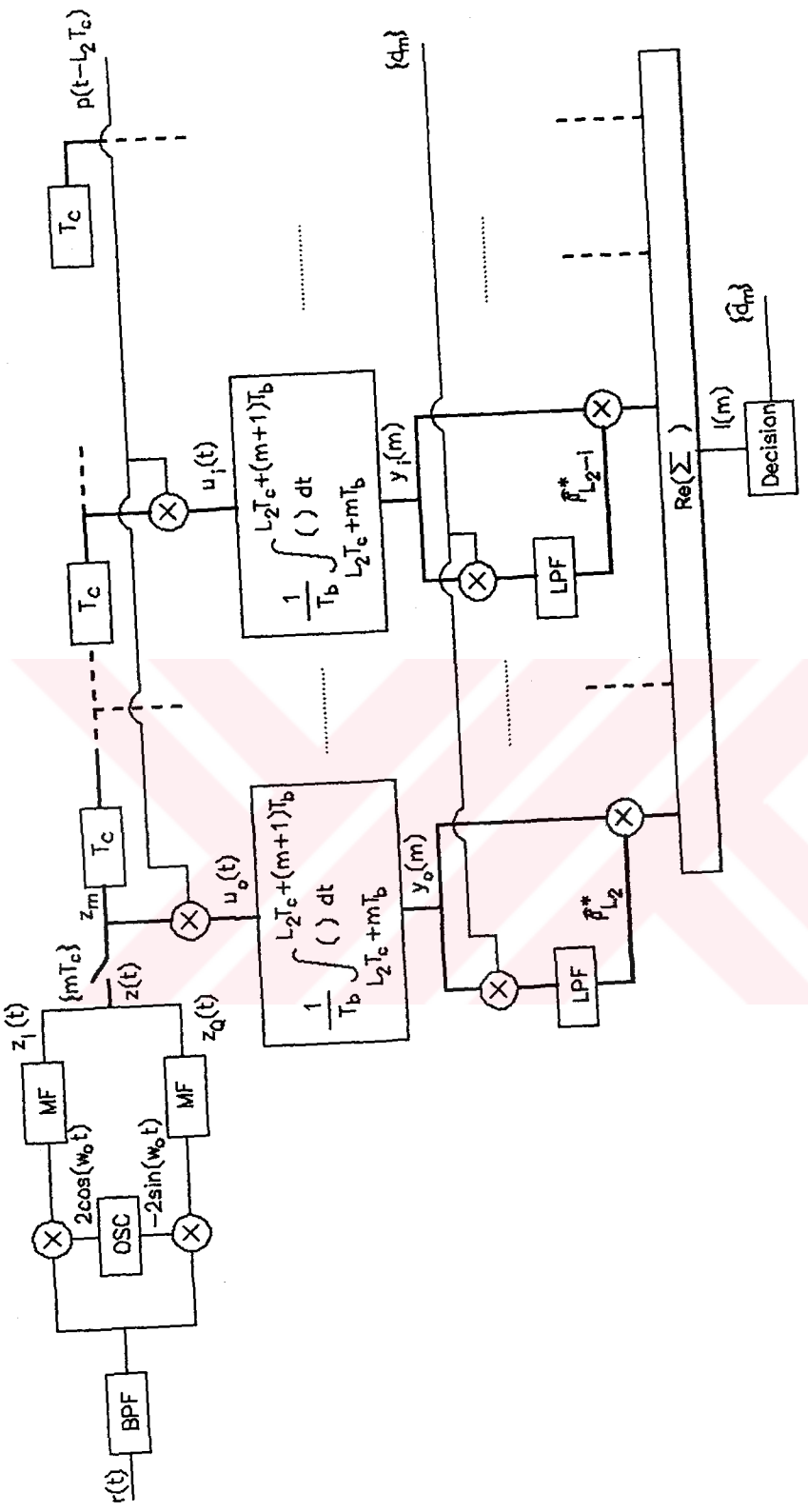

Figure 5.2. Block Diagram of the Receiver

Here, it is assumed that the interference from other emitters can be approximated as Gaussian although they are not. Nevertheless, this assumption becomes quite accurate if there is a large number of interferers and the interfering signals are uncorrelated with the desired signal and uncorrelated among themselves. Under these conditions, their sum can be approximated as Gaussian [6,16,17]. It should be noted that successive paths are assumed to have a delay difference equal to T_c. Thus, the bandwidth of the transmitted signal is near to $1/T_c$ which is the minimum intersymbol interference (ISI) free transmission bandwidth for PSK signals [9].

Since the transmitted signal s(t) is bandlimited, the received signal r(t) passes through a bandpass filter (BPF) having sufficient bandwidth to prevent signal distortion. Then, the filtered signal is quadrature demodulated by multiplying $2\cos(2\pi f_0 t)$ and $-2\sin(2\pi f_0 t)$. In order to avoid the intersymbol interference, the two matched filters with the impulse response g(-t) are used. Hence, the baseband (lowpass) equivalent of the received signal is obtained. The quadrature matched filter outputs are defined as a complex signal as

$$z(t) = z_I(t) + jz_Q(t) \tag{5.1.3}$$

and z(t) is expressed by

$$z(t) = \sum_{l=0}^{L} \beta_l \left[\sum_{k=-\infty}^{\infty} d_{[k/M]}\, p_k\, q(t-kT_c-lT_c) + \mu(t) \right] \tag{5.1.4}$$

where

$$\beta_l = a_l e^{j\phi_l} \quad (\phi_l = \theta_l - \omega_0 l T_c)$$

$$q(t) = g(t) \otimes g(-t)$$

$$\mu(t) = \eta(t) \otimes g(-t)$$

and where $\eta(t)$ represents the lowpass equivalent of n(t).

The other part of the receiver has a structure known as RAKE [9]. First of all z(t) is sampled at a rate of $1/T_c$ known as chip rate. The sampler output is expressed by

$$z_m = \sum_{l=0}^{L} \beta_l \left[\sum_{k=-\infty}^{\infty} d_{[k/M]}\, p_k\, q(mT_c - kT_c - lT_c) + \mu_m \right] \qquad (5.1.5)$$

where μ_m represents the sample of the lowpass equivalent of the noise.

In order to avoid the ISI, q(t) satisfies Nyquist's first criterion:

$$q(mT_c) = \begin{cases} 1 & m = 0 \\ 0 & \text{otherwise} \end{cases} \qquad (5.1.6)$$

Hence, z_m is simplified to

$$z_m = \sum_{l=0}^{L} \beta_l\, d_{\left[\frac{m-l}{M}\right]}\, p_{m-l} + \mu_m \qquad (5.1.7)$$

The sampled lowpass equivalent of the received signal z_m is passed through a tapped delay line with the tap spacing T_c. Thus, the multipath components corresponding to different paths are separated. The delayed version of z_m is defined as

$$z_{m-i} = \sum_{l=0}^{L} \beta_l\, d_{\left[\frac{m-i-l}{M}\right]}\, p_{m-i-l} + \mu_{m-i} \qquad (5.1.8)$$

where i denotes the i^{th} tap.

Then, the tapped signals are multiplied with a delayed version of the spreading sequence to despread it. Thus $u_i(t)$ shown in Fig. 5.2 can be expressed by

$$u_i(t) = z_i(t)\, p(t - L_2 T_c) \qquad (5.1.9)$$

or equivalently

$$u_i(t) = \sum_{l=0}^{L} \beta_l \sum_m \sum_r d_{\left[\frac{m-i-l}{M}\right]} p_{m-i-l} p_r \, \mathrm{rect}\left(\frac{t-mT_c}{T_c}\right) \mathrm{rect}\left(\frac{t-rT_c - L_2T_c}{T_c}\right)$$

$$+ \sum_m \sum_r \mu_{m-i} \, p_r \, \mathrm{rect}\left(\frac{t-mT_c}{T_c}\right) \mathrm{rect}\left(\frac{t-rT_c - L_2T_c}{T_c}\right)$$

(5.1.10)

where rect(x) is called rectangular function denoted as

$$\mathrm{rect}(x) = \begin{cases} 1 & 0<x\leq 1 \\ 0 & \text{otherwise} \end{cases}$$

Here, we assume an analog implementation of this part of the receiver. Thus all signals have staircase-like waveforms. The length of a delay line is proportional to the multipath spread of the channel. However, in a practical implementation, the complete span of the channel impulse response needs not to be covered by the RAKE receiver since it is generally vanishingly small at both ends. Therefore, the receiver is modified. In other words, it is assumed that the significant portion of the channel impulse response has the range from L_1^{st} to L_2^{nd} paths.

In the above Eq. 5.1.10, for rectangular matching

$r = m - L_2$

Then $u_i(t)$ becomes

$$u_i(t) = \sum_{l=0}^{L} \beta_l \sum_m d_{\left[\frac{m-i-l}{M}\right]} p_{m-i-l} \, p_{m-L_2} \, \mathrm{rect}\left(\frac{t-mT_c}{T_c}\right) + \sum_m \mu_{m-i} \, p_{m-L_2} \, \mathrm{rect}\left(\frac{t-mT_c}{T_c}\right)$$

(5.1.11)

Since $\{p_k\}$ is a binary $\{\pm 1\}$ sequence, $p^2_k = 1$, we have:

$$u_i(t) = \beta_{L_2-i} \sum_m d_{\left[\frac{m-L_2}{M}\right]} \text{rect}\left(\frac{t-mT_c}{T_c}\right) + \sum_{\substack{l=0 \\ l\neq L_2-i}}^{L} \beta_l \sum_m d_{\left[\frac{m-i-l}{M}\right]} p_{m-i-l}\, p_{m-L_2} \text{rect}\left(\frac{t-mT_c}{T_c}\right)$$

$$+ \sum_m \mu_{m-i}\, p_{m-L_2} \text{rect}\left(\frac{t-mT_c}{T_c}\right) \qquad (5.1.12)$$

The multiplication of $\{p_k\}$ and $\{p_l\}$, if $k \neq l$, is a new binary sequence, therefore it results in a signal-dependent self noise, which degrades the performance.

$u_i(t)$ can be written in a compact manner by including signal and noise terms:

$$u_i(t) = \beta_{L_2-i} \sum_k d_k \text{rect}\left(\frac{t-kT_b-L_2T_c}{T_b}\right) + \rho_i(t) \qquad (5.1.13)$$

where $\rho_i(t)$ is the total noise consisting of both self interferences and additive Gaussian noise (AWGN):

$$\rho_i(t) = \sum_{\substack{l=0 \\ l\neq L_2-i}}^{L} \beta_l \sum_k d_{\left[\frac{k-i-l}{M}\right]} p_{k-i-l}\, p_{k-L_2} \text{rect}\left(\frac{t-kT_c}{T_c}\right) + \sum_k \mu_{k-i}\, p_{k-L_2} \text{rect}\left(\frac{t-kT_c}{T_c}\right)$$

(5.1.14)

$u_i(t)$ is fed to an integrate and dump filter, which is used to reject higher frequency components from multiplication. The output of the filter is given by

$$y_i(m) = \frac{1}{T_b} \int_{L_2T_c+mT_b}^{L_2T_c+(m+1)T_b} u_i(t)\, dt \qquad (5.1.15)$$

In the derivation for the error probability of the RAKE receiver, the estimates of the channel tap weights are considered. There are many studies on this subject in the literature[5,8,15]. For example, in Pahlavan's work [8], he applied two ways to implement the channel estimator. One is to design a cross correlation to calculate channel parameters, and the second is to use the equalizer-like channel estimator, which is implemented by applying the least mean square (LMS) algorithm by Widrow [9]. The problem of channel parameter estimation was considered by Iltis[15]. He applied Kalman and extended Kalman filter (EKF) to obtain estimates .

Figure 5.2 illustrates a simple method for estimating the tap weights. We define channel tap coefficient β_l in complex form in Eq. 5.1.4. We want to estimate β^*_l thus, not only path amplitude is estimated but also the path phase shifts are compensated for.

In order to estimate the channel parameters β^*_l,the integrate and dump filter outputs are multiplied by the data sequence $\{d_m\}$ and passed through lowpass filters, whose bandwidths are proportional to Doppler spread of the channel, since Doppler spread reflects the rate of variation of the channel impulse response. Notice here that we assume the availability of the data sequence $\{d_m\}$ at the receiver; that is possible only in training portions of data. However, as it is usually done in the literature, one can assume that the probability of error, P_b is small enough during actual data transmission portions and a decision feedback mechanism can be used to supply the necessary signal.

Then, each integrate and dump filter output is multiplied by the complex conjugate of the corresponding estimated channel parameter so that the phase shift in the channel can be compensated for and the signal is weighted by a factor that is proportional to the path strength.

After the complex-valued weighting operation is carried out, the outputs are summed to obtain optimal detection. This process is the principle of a maximal ratio combiner by Brennan (1959) [9]. The best reduction of fading is obtained by this kind of combination. The weighting is desirable for maximal ratio combining.

For optimal detection, $y_i(m)$ are linearly combined using $\hat{\beta}_1^*$ to obtain the decision variable, l(m):

$$l(m) = \mathrm{Re}\left\{ \sum_{i=0}^{L_2-L_1} y_i(m)\, \hat{\beta}^*_{L_2-i} \right\} \qquad (5.1.16)$$

It should be noted that only the real part of the maximal ratio combiner is considered since the imaginary part does not contain (ideally) the signal component.

Finally, l(m) is hardlimited to obtain the detected bit $\hat{d}_m$.

5.2 Performance Analysis

This section presents the performance analysis of the RAKE receiver described in the previous section.

We described the system model in the previous section. By using figures and equations in that section, we will derive the probability of error function for a given set of channel parameters $\{\beta_k\}$.

The integrate and dump filter output $y_i(m)$ shown in Fig. 5.2 is given by Eq. 5.1.15. Evaluating the integral and separating the term that belongs to the tap of interest and the fact that $p^2_k = 1$, we have :

$$y_i(m) = \beta_{L_2-i} d_m + \vartheta_i(m) \qquad (5.2.1)$$

where $\upsilon_i(m)$ represents the total noise consisting both additive noise and interference components and is equal to

$$\vartheta_i(m) = \frac{1}{M} \sum_{\substack{l=0 \\ l \neq L_2-i}}^{L} \beta_l \sum_{r=0}^{M-1} d_{\left[\frac{mM+r+L_2-i-l}{M}\right]} p_{mM+r+L_2-i-l}\, p_{mM+r}$$

$$+ \frac{1}{M} \sum_{r=0}^{M-1} \mu_{mM+r+L_2-i}\, p_{mM+r} \qquad (5.2.2)$$

As mentioned earlier, the integrate and dump filter output $y_i(m)$ is multiplied by the data sequence $\{d_m\}$ to estimate the channel parameters β_l. Thus, the resultant signal is given by

$$y_i(m)d_m = \beta_{L_2-i} + \vartheta_i(m)d_m \qquad (5.2.3)$$

As shown Fig. 5.2 this signal is applied to a lowpass filter (LPF). Since $\{d_k\}$, $\{p_k\}$ and $\{\mu_k\}$ are white,independent zero mean sequences the mean of second term in Eq. 5.2.3 is zero. It is assumed that the rate of variations for β_k is small as compared to the bandwidth of the LPF. Therefore the output of the LPF can be expressed by

$$\hat{\beta}_{L_2-i} = \beta_{L_2-i} + a_i(m) \qquad (5.2.4)$$

where $a_i(m)$ is a zero mean process that is interpreted as the estimation error for β_{L_2-k}

Then the signal $y_i(m)$ is multiplied by the complex conjugate of the estimated channel parameters, $\hat{\beta}^*_{L_2-i}$.

Finally the receiver collects the signal energy from the received signal paths with in the span of the delay line. The decision variable l(m) is obtained from Eq. 5.1.16, Eq. 5.2.1 and Eq. 5.2.4 as

$$l(m) = \sum_{i=0}^{L_2-L_1} \left|\beta_{L_2-i}\right|^2 d_m + v_m \qquad (5.2.5)$$

where

$$v_m = \mathrm{Re}\left\{ \sum_{i=0}^{L_2-L_1} w_i(m) \right\} \qquad (5.2.6)$$

and

$$w_i(m) = \beta_{L_2-i} d_m a_i^*(m) + \beta_{L_2-i}^* \vartheta_i(m) + \vartheta_i(m) a_i^*(m) \qquad (5.2.7)$$

5.2.1 Probability of Error

It is seen that in Eq. 5.2.6 v_m is a combination of many terms. Their distribution is not actually Gaussian. The estimation error sequence $\{a_k\}$ is a narrowband signal compared to $\{\upsilon_k\}$ since $\{a_k\}$ is lowpass filtered. The other sequence, $\{d_k\}$, is a zero mean and independent of $\{a_k\}$ and $\{\upsilon_k\}$. Thus, they are uncorrelated among themselves and their sum can be approximated as Gaussian [20]. Hence, in Eq. 5.2.6, v_m is assumed to be a zero mean approximately Gaussian random variable with standard deviation, σ^2.

The probability of error, P_b is given by

$$P_b = \sum P(E/H_i)P(H_i) \qquad (5.2.1.1)$$

where $P(E/H_i)$ is the probability of error given hypothesis H_i.

Since data bits $\{d_k\}$ are equally likely and the problem is perfectly symmetric, it is seen that

$$P_b = P(E/H_0) \qquad (5.2.1.2)$$

For an ideal detector and for BPSK signalling, the probability of error [9] is

$$P(E/H_0) = P\left(v_m > \sum_{i=0}^{L_2-L_1} \left|\beta_{L_2-i}\right|^2\right) \qquad (5.2.1.3)$$

$$P_b = \frac{1}{2}\operatorname{erfc}\left(\frac{\sum_{i=0}^{L_2-L_1} \left|\beta_{L_2-i}\right|^2}{\sqrt{2\sigma^2}}\right) \qquad (5.2.1.4)$$

where

$$\operatorname{erfc}(x) = \frac{2}{\sqrt{\pi}} \int_x^{\infty} e^{-t^2} dt$$

In order to obtain P_b, it is necessary to compute σ^2.

5.2.2 Noise Variance

Let $\{x_i(m)\}$ and $\{y_i(m)\}$ be two jointly wide sense stationary random process. We define the following functions :

$$\phi_{x,y}(k) = E\{x(m+k)y(m)\} \qquad (5.2.2.1)$$

$$\psi_{x,y}(k) = E\{x(m+k)y^*(m)\} \qquad (5.2.2.2)$$

where $E\{.\}$ is the expected value operator. It should be noticed that Eq.5.2.2.2 is conventional definition of the crosscorrelation function. Since v_m is a zero mean random variable, σ^2 can be expressed as

$$\sigma^2 = E\left\{v_m^2\right\}$$

$$\sigma^2 = \frac{1}{2}\mathrm{Re}\left\{\sum_{i=0}^{L_2-L_1}\sum_{j=0}^{L_2-L_1} E\left\{w_i(m)\, w_j(m)\right\}\right\} + \frac{1}{2}\sum_{i=0}^{L_2-L_1}\sum_{j=0}^{L_2-L_1} E\left\{w_i(m)\, w_j^*(m)\right\} \quad (5.2.2.3)$$

By the Eq. 5.2.2.1 and 5.2.2.2,σ^2 is simplified to

$$\sigma^2 = \frac{1}{2}\mathrm{Re}\left\{\sum_{i=0}^{L_2-L_1}\sum_{j=0}^{L_2-L_1} \phi_{w_i w_j}(0)\right\} + \frac{1}{2}\sum_{i=0}^{L_2-L_1}\sum_{j=0}^{L_2-L_1} \psi_{w_i w_j}(0) \quad (5.2.2.4)$$

σ^2 can be obtained by computing $\phi_{w_i w_j}(0)$ and $\psi_{w_i w_j}(0)$. Now, let us start with $\phi_{w_i w_j}(0)$.

From Eq. 5.2.7 and Eq. 5.2.2.1

$$\begin{aligned}\phi_{w_i w_j}(0) = {} & \beta_{L_2-i}\beta_{L_2-j}\phi^*_{a_i a_j}(0) + \beta^*_{L_2-i}\beta^*_{L_2-j}\phi_{\vartheta_i\vartheta_j}(0) + \phi^*_{a_i a_j}(0)\phi_{\vartheta_i\vartheta_j}(0) \\ & + \beta_{L_2-i}\beta^*_{L_2-j}E\left\{a_i^*(m)\vartheta_j(m)d_m\right\} + \beta_{L_2-i}E\left\{a_i^*(m)a_j^*(m)d_m\vartheta_j(m)\right\} \\ & + \beta^*_{L_2-i}\beta_{L_2-j}E\left\{a_j^*(m)\vartheta_i(m)d_m\right\} + \beta^*_{L_2-i}E\left\{\vartheta_i(m)\vartheta_j(m)a_j^*(m)\right\} \\ & + \beta_{L_2-j}E\left\{a_i^*(m)a_j^*(m)\vartheta_i(m)d_m\right\} + \beta^*_{L_2-j}E\left\{\vartheta_i(m)\vartheta_j(m)a_i^*(m)\right\}\end{aligned} \quad (5.2.2.5)$$

Considering that the data sequence $\{d_k\}$, spreading sequence $\{p_k\}$ and the additive noise $\{\mu_k\}$ are all independent sequences, significant simplifications are possible. It is assumed that the the LPF bandwidth is much smaller than the bit rate.

Since the estimation error sequence $\{a_k\}$ is lowpass filtered and $\{\upsilon_i(m)\}$ is a wideband sequence, they are assumed as uncorrelated sequences. Besides, $\{a_k\}$ is almost independent of $\{d_k\}$ and $\{p_k\}$. Therefore, in Eq. 5.2.2.5, only first three terms affect the sum. Hence, $\phi_{w_iw_j}(0)$ is simplified to

$$\phi_{w_iw_j}(0) = \beta_{L_2\text{-}i}\beta_{L_2\text{-}j}\,\phi^*_{a_ia_j}(0) + \beta^*_{L_2\text{-}i}\beta^*_{L_2\text{-}j}\phi_{\vartheta_i\vartheta_j}(0) + \phi^*_{a_ia_j}(0)\phi_{\vartheta_i\vartheta_j}(0) \qquad (5.2.2.6)$$

Secondly, we should evaluate $\psi_{w_iw_j}(0)$. From Eq. 5.2.7 and Eq.5.2.2.2

$$\begin{aligned}\psi_{w_iw_j}(0) = {} & \beta_{L_2\text{-}i}\beta^*_{L_2\text{-}j}\,\psi^*_{a_ia_j}(0) + \beta^*_{L_2\text{-}i}\beta_{L_2\text{-}j}\psi_{\vartheta_i\vartheta_j}(0) + \psi^*_{a_ia_j}(0)\psi_{\vartheta_i\vartheta_j}(0) \\ & + \beta_{L_2\text{-}i}\beta_{L_2\text{-}j}E\left\{a_i^*(m)\vartheta_j^*(m)d_m\right\} + \beta_{L_2\text{-}i}E\left\{a_i^*(m)\vartheta_j^*(m)a_j(m)d_m\right\} \\ & + \beta^*_{L_2\text{-}i}\beta^*_{L_2\text{-}j}E\left\{\vartheta_i(m)a_j(m)d_m\right\} + \beta^*_{L_2\text{-}i}E\left\{\vartheta_i(m)\vartheta_j^*(m)a_j(m)\right\} \\ & + \beta^*_{L_2\text{-}j}E\left\{\vartheta_i(m)d_m a_i^*(m)a_j(m)\right\} + \beta_{L_2\text{-}j}E\left\{\vartheta_i(m)\vartheta_j^*(m)a_i^*(m)\right\}\end{aligned} \qquad (5.2.2.7)$$

Since the same reason explained for $\phi_{w_iw_j}(0)$ is valid for $\psi_{w_iw_j}(0)$, the expression takes the form

$$\psi_{w_iw_j}(0) = \beta_{L_2\text{-}i}\beta^*_{L_2\text{-}j}\psi^*_{a_ia_j}(0) + \beta^*_{L_2\text{-}i}\beta_{L_2\text{-}j}\psi_{\vartheta_i\vartheta_j}(0) + \psi^*_{a_ia_j}(0)\psi_{\vartheta_i\vartheta_j}(0) \qquad (5.2.2.8)$$

In order to obtain σ^2, we have to find expressions for $\phi_{\vartheta_i\vartheta_j}$, $\phi_{a_ia_j}$, $\psi_{\vartheta_i\vartheta_j}$ and $\psi^*_{a_ia_j}$.

The channel noise $\upsilon_i(m)$ given in Eq.5.2.2 is rewritten to compute $\phi_{\vartheta_i\vartheta_j}$ or $\psi_{\vartheta_i\vartheta_j}$ easily. Hence,

$$\vartheta_i(m) = \gamma_i(m) + \eta_i(m) \tag{5.2.2.9}$$

where

$$\gamma_i(m) = \frac{1}{M} \sum_{\substack{l=0 \\ l \neq L_2-i}}^{L} \beta_l \sum_{r=0}^{M-1} d\left[\frac{mM+r+L_2-i-l}{M}\right] p_{mM+r+L_2-i-l}\, p_{mM+r} \tag{5.2.2.10}$$

and

$$\eta_i(m) = \frac{1}{M} \sum_{r=0}^{M-1} \mu_{mM+r+L_2-i}\, p_{mM+r} \tag{5.2.2.11}$$

Since $\{\gamma_i(m)\}$ and $\{\eta_i(m)\}$ are uncorrelated zero mean sequences, $\phi_{\vartheta_i\vartheta_j}(0)$ can be expressed by

$$\phi_{\vartheta_i\vartheta_j}(0) = \phi_{\gamma_i\gamma_j}(0) + \phi_{\eta_i\eta_j}(0) \tag{5.2.2.12}$$

Then, we can evaluate $\phi_{\gamma_i\gamma_j}(0)$ and $\phi_{\eta_i\eta_j}(0)$ separately.

$$\phi_{\eta_i\eta_j}(0) = \frac{1}{M^2} \sum_{r=0}^{M-1} \sum_{r'=0}^{M-1} E\left\{\mu_{mM+r+L_2-i}\, \mu_{mM+r'+L_2-j}\, p_{mM+r}\, p_{mM+r'}\right\} \tag{5.2.2.13}$$

Since $\{p_k\}$ and $\{\mu_k\}$ are uncorrelated sequences, then the expectations are separated.

$$\phi_{\eta_i\eta_j}(0) = \frac{1}{M^2} \sum_{r=0}^{M-1} \sum_{r'=0}^{M-1} E\left\{\mu_{mM+r+L_2-i}\, \mu_{mM+r'+L_2-j}\right\} E\left\{p_{mM+r}\, p_{mM+r'}\right\} \tag{5.2.2.14}$$

The expected value of the product of two random variables differs from zero when they are same.Thus the indices of $\{p_k\}$ should be equal.That is

$$E\{p_{mM+r}\, p_{mM+r'}\} = \begin{Bmatrix} 1 \text{ ,} r=r' \\ 0 \text{ ,otherwise} \end{Bmatrix}$$

Hence, one of the summations is dropped. It is easily seen that

$$E\{\mu_{mM+r+L_2-i}\, \mu_{mM+r'+L_2-j}\} = 0 \qquad (5.2.2.15)$$

Then, $\phi_{\eta_i\eta_j}(0) = 0$.

Now, we consider only $\phi_{\gamma_i\gamma_j}(0)$. The result for $\phi_{\vartheta_i\vartheta_j}(0)$ is

$$\phi_{\vartheta_i\vartheta_j}(0) = \frac{1}{M^2} \sum_{\substack{l=0 \\ l\neq L_2-i}}^{L} \sum_{\substack{l'=0 \\ l'\neq L_2-j}}^{L} \beta_l\beta_{l'} \sum_{r=0}^{M-1} \sum_{r'=0}^{M-1} E\left\{d_{\left\lfloor \frac{mM+r+L_2-i-l}{M} \right\rfloor} d_{\frac{mM+r'+L_2-j-l'}{M}}\right\}$$

$$* E\{p_{mM+r+L_2-i-l} p_{mM+r} p_{mM+r'+L_2-j-l'} p_{mM+r'}\} \qquad (5.2.2.16)$$

Making use of the assumptions earlier and forming the products, we apply a case by case procedure in determining the expected values of the product of four binary random variables.

We will check pairwise equations by examining the indices of $\{p_k\}$. The cases are below :

1. p_{mM+r+L_2-i-l} , p_{mM+r} and $p_{mM+r'+L_2-j-l'}$, $p_{mM+r'}$

   i) $mM+r+L_2-i-l = mM+r$
   ii) $mM+r'+L_2-j-l' = mM+r'$

where we define the function b(.) for convenience,

$$b(k) = \sum_{r=0}^{M-1} E\left\{ d_{\left[\frac{r+k}{M}\right]} d_0 \right\} \qquad (5.2.2.18)$$

In computations, this function is computed only for once by a range analysis on the index of the sum, and it is stored for future calculations.

Next, we consider $\phi_{a_i a_j}(0)$. Let $x_i(m)= \upsilon_i(m)*d_m$ be the input of the estimator LPF's. The output of filter is $a_j(m)$. The power spectral density of $\{a_k\}$, $\Phi_{a_i a_j}(\omega)$ is given by

$$\Phi_{a_i a_j}(\omega) = |H(e^{j\omega})|^2 \Phi_{x_i x_j}(\omega) \qquad (5.2.2.19)$$

where $H(e^{jw})$ is the frequency response of the LPF.

It is noticed that $x_i(m)$ is a wideband signal, whereas $H(e^{jw})$ has a very narrow bandwidth which is, in fact, proportional to the Doppler spread of the channel and it has unity DC gain. Hence,

$$\Phi_{a_i a_j}(\omega) \cong |H(e^{j\omega})|^2 \Phi_{x_i x_j}(0) \qquad (5.2.2.20)$$

by taking the inverse Fourier transform, and evaluating at $\omega=0$, we have:

$$\phi_{a_i a_j}(0) = \frac{\omega_c}{\pi} \Phi_{x_i x_j}(0) \qquad (5.2.2.21)$$

where ω_c is the noise equivalent bandwidth of the lowpass filter,

$$\omega_c = \int_0^{\infty} |H(e^{j\omega})|^2 \, d\omega \qquad (5.2.2.22)$$

Taking account of the fact that digital frequency 2π corresponds to analog frequency $1/T_b$ then $\omega_c = 2\pi f_d T_b$, where f_d is analog noise equivalent bandwidth of the LPF. Then, using discrete time Fourier transform properties:

$$\phi_{a_i a_j}(0) = 2f_d T_b \sum_k \phi_{x_i x_j}(k) \qquad (5.2.2.23)$$

Now, we should find $\phi_{x_i x_j}(k)$. It can be found in a similar manner as explained above. Briefly,

$$\text{let} \quad x_i(m) = \gamma_i(m) + \eta_i(m)$$

where

$$\gamma_i(m) = \frac{1}{M} \sum_{\substack{l=0 \\ l \neq L_2-i}}^{L} B_l \sum_{r=0}^{M-1} d_{\left[\frac{mM+r+L_2-i-l}{M}\right]} d_m p_{mM+r+L_2-i-l} p_{mM+r} \qquad (5.2.2.24)$$

and

$$\eta_i(m) = \frac{1}{M} \sum_{r=0}^{M-1} \mu_{mM+r+L_2-i-l} d_m p_{mM+r} \qquad (5.2.2.25)$$

Since $\{\gamma_k\}$ and $\{\eta_k\}$ are uncorrelated sequences, we have:

$$\phi_{x_i x_j}(k) = \phi_{\gamma_i \gamma_j}(k) + \phi_{\eta_i \eta_j}(k) \qquad (5.2.2.26)$$

Firstly, $\phi_{\eta_i \eta_j}(k)$, can be examined.

$$\phi_{\eta_i \eta_j}(k) = \frac{1}{M^2} \sum_{r=0}^{M-1} \sum_{r'=0}^{M-1} E\{\mu_{(m+k)M+r+L_2-i} \mu_{mM+r'+L_2-j}\} E\{d_{(m+k)} d_m\}$$

$$* E\{p_{(m+k)M+r} p_{mM+r'}\} \qquad (5.2.2.27)$$

Considering the expected values separately, the conditions are obtained as follows:

1. $E\{d_{(m+k)}\, d_m\} = 1 \qquad \text{if } k = 0$
2. $E\{p_{(m+k)M+r} p_{mM+r'}\} = 1 \qquad \text{if } r'-r = kM$

Since $0 \le r \le M-1$ and $0 \le r' \le M-1$, the second condition is satisfied if k=0. Then,

$$\phi_{\eta_i\eta_j}(k) = \frac{1}{M^2} \sum_{r=0}^{M-1} E\{\mu_{mM+r+L_2-i}\, \mu_{mM+r'+L_2-j}\}\, \delta_k \qquad (5.2.2.28)$$

and we know that $E\{\mu_{k+1}\mu_k\} = 0$, $\phi_{\eta_i\eta_j}(k) = 0$

Therefore, only $\phi_{\gamma_i\gamma_j}(k)$ affects the computation of $\phi_{x_ix_j}(k)$. Henceforth, we use $\phi_{x_ix_j}(k)$ instead of $\phi_{\gamma_i\gamma_j}(k)$.

$$\phi_{x_ix_j}(k) = \frac{1}{M^2} \sum_{\substack{l=0 \\ l \ne L_2-i}}^{L} \sum_{\substack{l'=0 \\ l' \ne L_2-j}}^{L} \beta_l\, \beta_{l'}$$

$$* \sum_{r=0}^{M-1} \sum_{r'=0}^{M-1} E\left\{ d_{\left\lfloor \frac{(m+k)M+r+L_2-i-l}{M} \right\rfloor}\, d_{(m+k)}\, d_{\left\lfloor \frac{mM+r'+L_2-j-l'}{M} \right\rfloor}\, d_m \right\}$$

$$* E\{p_{(m+k)M+r+L_2-i-l}\, p_{(m+k)M+r}\, p_{mM+r'+L_2-j-l'}\, p_{mM+r'}\}$$

(5.2.2.29)

A case by case procedure follows for evaluation:

1. $p_{(m+k)M+r+L_2-i-l}$, $p_{(m+k)M+r}$ and $p_{mM+r'+L_2-j-l'}$, $p_{mM+r'}$

i) $(m+k)M+r+L_2-i-l = (m+k)M+r$

ii) $mM+r'+L_2-j-l' = mM+r'$

These equalities are not possible because of the conditions $l \neq L_2-i$ and $l' \neq L_2-j$.

2. $p_{(m+k)M+r}$, $p_{mM+r'}$ and $p_{(m+k)M+r+L_2-i-l}$, $p_{mM+r'L_2-j-l'}$

i) $(m+k)M+r = mM+r'$

ii) $(m+k)M+r+L_2-i-l = mM+r'+L_2-j-l'$

From the first equality, $r'-r=kM$ is obtained. However, r' and r can take only values between 0 and M-1, k should be zero. Then,

$k = 0$

$r = r'$

$l' = l+i-j$ is obtained from the second equality.

3. $p_{(m+k)M+r+L_2-i-l}$, $p_{mM+r'}$ and $p_{mM+r'+L_2-j-l'}$, $p_{(m+k)M+r}$

i) $(m+k)M+r+L_2-i-l = mM+r'$

ii) $mM+r'+L_2-j-l' = (m+k)M+r$

by solving these equations, we have:

$r' = kM+r+L_2-i-l$,

$l' = 2L_2-i-j-l$

Putting into these conditions found above in the Eq. 5.2.2.29, $\phi_{x_i x_j}(k)$ becomes

$$\phi_{x_i x_j}(k) = \frac{1}{M} \sum_{\substack{l=0 \\ l \neq L_2 - i}}^{L} \beta_l \beta_{l+i-j} \delta_k$$

$$+ \frac{1}{M^2} \sum_{\substack{l=0 \\ l \neq L_2 - i}}^{L} \beta_l \beta_{2L_2 - i - j - l} \sum_{r=0}^{M-1} E\left\{ d_{\left\lfloor \frac{(m+k)M+r+L_2-i-l}{M} \right\rfloor} d_{(m+k)} d_{\left\lfloor \frac{(m+k)M+r}{M} \right\rfloor} d_m \right\}$$

(5.2.2.30)

Since $0 \leq r \leq M-1$, $d_{\left\lfloor \frac{(m+k)M+r}{M} \right\rfloor}$ is always $d_{(m+k)}$ and so $d^2_{(m+k)} = 1$. Hence,

$$\phi_{x_i x_j}(k) = \frac{1}{M} \sum_{\substack{l=0 \\ l \neq L_2 - i}}^{L} \beta_l \beta_{l+i-j} \delta_k + \frac{1}{M^2} \sum_{\substack{l=0 \\ l \neq L_2 - i}}^{L} \beta_l \beta_{2L_2 - i - j - l} b(kM + L_2 - i - l)$$

(5.2.2.31)

It is noticed that due to definition of b(.), $b(kM+L_2-i-l)$ has a value different than zero if $-1 \leq k \leq 1$, and thus the range of k is limited. The approximate result for $\phi_{a_i a_j}(0)$ is given by

$$\phi_{a_i a_j}(0) \cong \frac{2}{M} f_d T_b \left[\sum_{\substack{l=0 \\ l \neq L_2 - i}}^{L} \beta_l \beta_{l+i-j} + \frac{1}{M} \sum_{k=-1}^{1} \sum_{\substack{l=0 \\ l \neq L_2 - i}}^{L} \beta_l \beta_{2L_2 - i - j - l} b(kM + L_2 - i - l) \right]$$

(5.2.2.32)

Finally, the ψ terms are determined easily by considering that they differ from the f functions only in some components will be replaced by their complex conjugates. functions also have additive noise terms whose definitions can be found in Appendix A. The results for ψ terms are:

$$\psi_{\vartheta_i\vartheta_j}(0) = \frac{1}{M}\left[2N_0\delta_{ij} + \sum_{\substack{l=0 \\ l\neq L_2-i}}^{L} \beta_l \beta^*_{l+i-j} + \frac{1}{M}\sum_{\substack{l=0 \\ l\neq L_2-i}}^{L} \beta_l \beta^*_{2L_2-i-j-l}\, b(L_2-i-l)\right]$$

(5.2.2.33)

$$\psi^*_{a_i a_j}(0) = \frac{2f_d T_b}{M}\left[2N_0\delta_{ij} + \sum_{\substack{l=0 \\ l\neq L_2-i}}^{L} \beta^*_l \beta_{l+i-j}\right]$$

$$\left[+ \frac{1}{M}\sum_{k=-1}^{1}\sum_{\substack{l=0 \\ l\neq L_2-i}}^{L} \beta^*_l \beta_{2L_2-i-j-l}\, b(kM+L_2-i-l)\right]$$

(5.2.2.34)

In summary, in order to compute P_b from Eq. 5.2.1.4, Eq. 5.2.2.17, Eq. 5.2.2.32 Eq. 5.2.2.33 and Eq. 5.2.2.34 will be evaluated first and then by making use of Eq. 5.2.2.6 and Eq. 5.2.2.8, σ^2 is computed.

CHAPTER VI

SIMULATION AND RESULTS

This chapter presents the results obtained using a computer simulation program. The chapter is divided into the following two main sections:

1) Simulation Model
2) Results

First, the simulation model will be discussed and simulation parameters will be defined. In the second section, the results of the performance of the RAKE receiver will be explained.

6.1 Simulation Model

As explained in Chapter 4, the channel impulse response profiles are generated in the simulation program, written in FORTRAN IV [1]. In the simulation, we generate :

1) a set of arrival times $\{t_k\}$
2) a set of amplitudes $\{a_k\}$
3) a set of phases $\{\theta_k\}$

The distance between the samples is chosen as 3 feet which represents the displacements of the mobile. As mentioned before, the original program generates the impulse response with a resolution of 100 nsec and this corresponds to a RF

bandwidth of 10 MHz. However, the performance analysis of smaller bandwidths are needed in simulations. This problem is solved as suggested in [5], by complex addition of the path phasors in adjacent 100 nsec intervals. This is explained in the following manner:

The paths are resolvable if

$$|t_k - t_l| \geq 1/W \quad \text{for all } k \neq l \tag{6.1.1}$$

where W is the transmission bandwidth, $\{t_k\}$ and $\{t_l\}$ represent the arrival times. When two or more paths arrive within (1/W) sec, they will combine and only a single path will be observed, i.e.,

$$|t_k - t_l| < 1/W \tag{6.1.2}$$

then, the strength/phase combination is given by

$$a_m \exp(j\theta_m) = a_k \exp(j\theta_k) + a_l \exp(j\theta_l) \tag{6.1.3}$$

In our simulations, for example, vectorial sums of 10 successive phasors from the 10 MHz response are formed to yield the path phasors for 1 MHz RF bandwidth.

The total noise variance, consisting of additive Gaussian noise and interference, and the probability of error function derived in Chapter 5 are computed by a computer program implemented in PASCAL. In the simulations, we used combinations of the following sets of system parameters :

f_c	= Chip Rate	= {1,2}	(MHz),
f_b	= Bit Rate	= {10,20,50,100}	(Kbps),
f_d	= LPF BW	= {0,10,30,60,120,200,300}	(Hz),
E_b/N_o	= SNR	= {3,4,6,8,10,12,15}	(dB).

Power control in mobile transmitters is used to compensate for changes in signal level due to path loss variations and fading. The power control is simulated for two cases :

i) Slow power control : The average E_b / N_o is set to a desired value for 150 profiles.

ii) Perfect power control : At each profile E_b / N_o is constant at a certain value.

Since we utilized different bandwidths in our simulations, the length of the tapped delay line (TDL) in the RAKE receiver was varied among a set of values. We note that the maximum length of the impulse response of the simulated radio channel is about 7 microseconds. Since the multipath channel is modeled as a $T_c = 1/W$ (W is RF bandwidth) spaced TDL, the maximum length of TDL is 75 for 10 MHz RF bandwidths. Under this consideration, for 1 and 2 MHz RF bandwidths, TDL has a length at most 7 and 15 respectively. In the simulations, the probability of error is computed for different spans of TDL.

As mentioned in Chapter 4 , the estimator LPF bandwidth is proportional to the Doppler spread of the channel, as the Doppler spread is related to the rate of variation of the channel impulse response. It is stated in [1] that a 3 feet sample separation is suitable to illustrate the variations with respect to movements. We assume that a vehicle moves at a speed of 50 km/hr. Then, taking into account the necessary spatial sampling interval of 3 feet, it can be found that the Doppler spread of the channel is about 15 Hz. In simulations, different LPF bandwidths are chosen to see the effect on the probability of error.

The performance of the RAKE receiver is also computed for various bit rates.

Finally, the most important feature in mobile communications, CDMA capacity, is evaluated for single cell and multicell cases by using the formula given in Chapter 3. The capacity is computed for 1 and 2 MHz RF bandwidths.

6.2 Results

In this section, the simulation results are investigated. The system parameters are changed, and their effects on the performance of the RAKE receiver are observed. The results are illustrated in the figures. In order to evaluate the performance of our simulation model, the number of profiles generated is chosen as 150, which is sufficient to illustrate the mobile movement. If the number of profiles increases, it will require more execution time for the simulation program.

6.2.1 Power Control

As mentioned before, power control is an important feature of spread spectrum systems. Fig. 6.1 and Fig. 6.2 depicts the probability of bit error P_b as a function of E_b/N_o for f_c = 1 and 2 MHz respectively. In the figures, perfect power control and slow power control are illustrated. We assume that full length tapped delay line (TDL) is used and $f_d = 0$ (very low speed). It is seen that for a constant E_b / N_o, there is a vast difference between P_b of perfect power control and P_b of slow power control. For example, when $E_b / N_o = 10$ dB, $P_b = 6*10^{-2}$ for slow power control, $P_b = 2*10^{-4}$ for perfect power control, as seen in Fig. 6.1. Therefore we can say that if only a slow power control is available CDMA spread spectrum systems degrade significantly.

6.2.2 Bit Rates

Fig. 6.3 and Fig. 6.4 illustrate P_b as a function of E_b/N_o for f_c = 1 and 2 MHz for various bit rates. In the simulations full length RAKE receiver and $f_d = 0$ are used. For f_c = 1 MHz, P_b variations in Fig. 6.3 are more pronounced than that for f_c = 2 MHz in Fig. 6.4. As shown in the figures, the higher bit rate degrades P_b since if bit rate increases, the spreading factor M decreases proportionally and thus noise level (including self interference and white noise) gets higher.

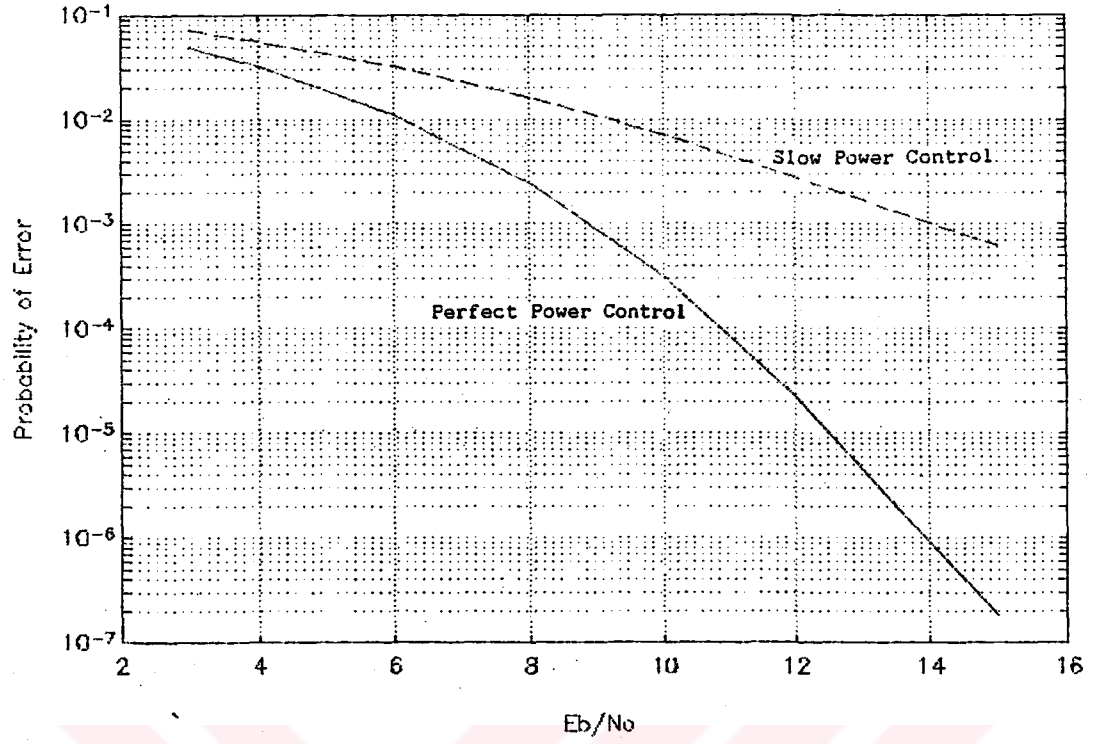

Figure 6.1. P_b vs. E_b / N_o for f_c=1 MHz, f_d=0

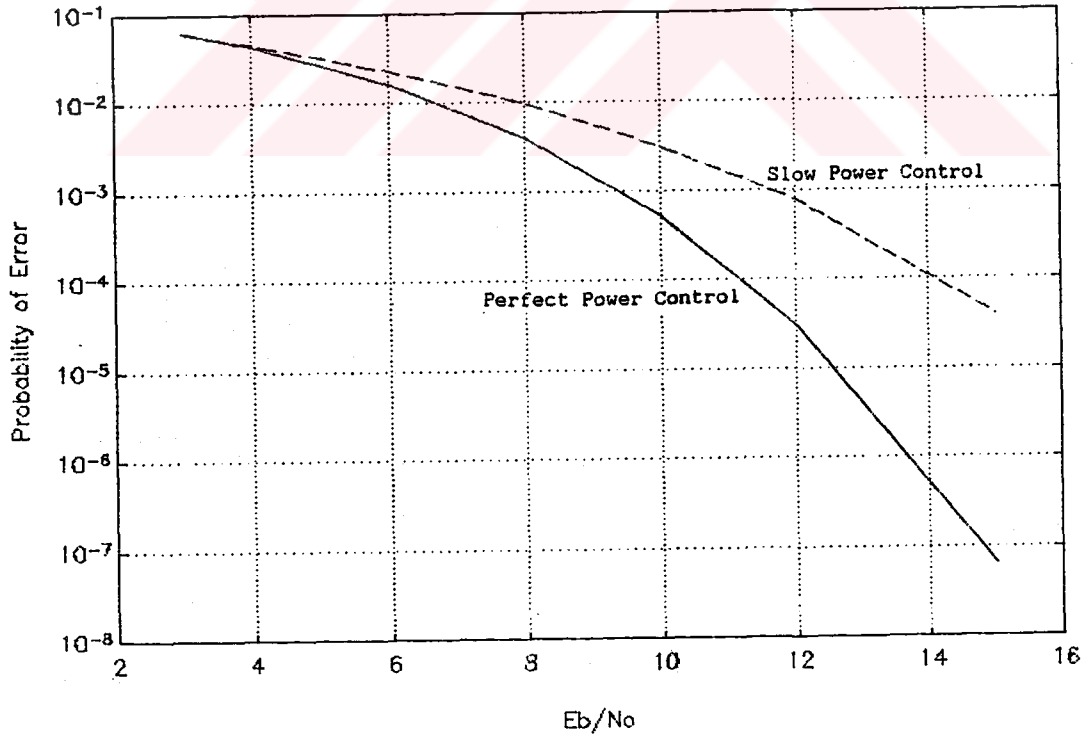

Figure 6.2. P_b vs. E_b / N_o for f_c=2 MHz, f_d=0

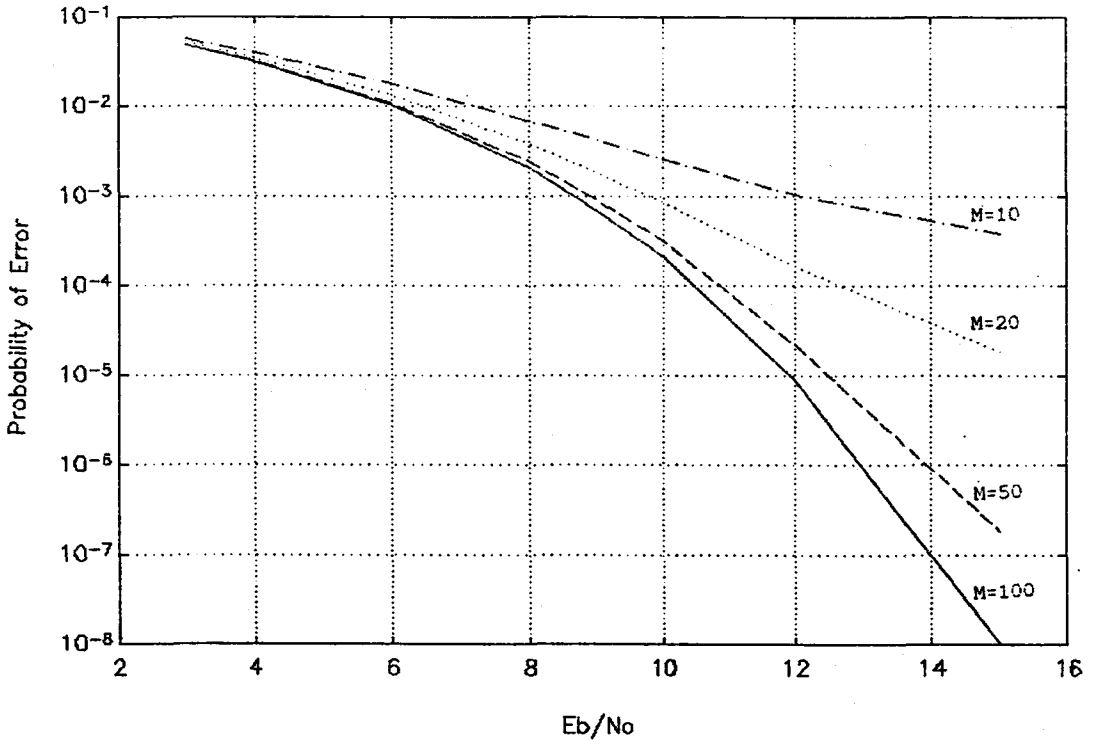

Figure 6.3. P_b vs. E_b / N_o for f_c=1 MHz, f_d=0

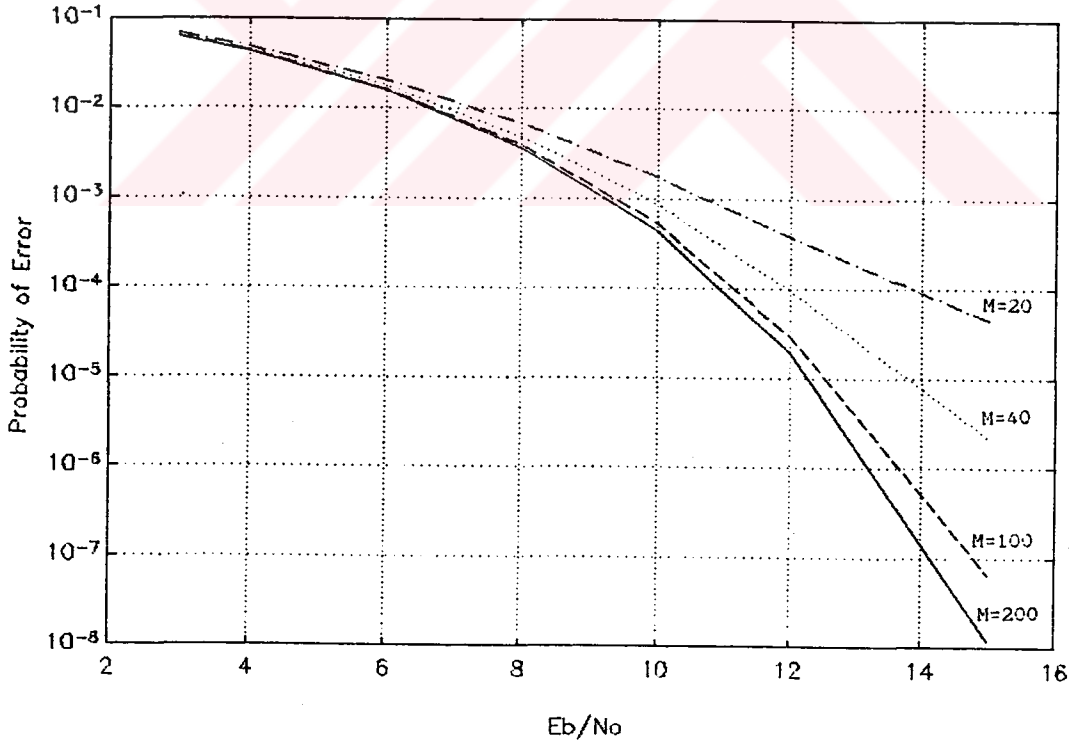

Figure 6.4. P_b vs. E_b / N_o for f_c=2 MHz, f_d=0

6.2.3 CDMA Capacity

The CDMA capacity for single cell and multicell operation and with perfect power control in the mobiles were derived in Chapter 3. By using Eq.3.4.1.7 and Eq.3.4.2.3, the capacities for both cases are calculated. We note that although E_b/N_o is a constant for a specified P_b ideally, it does change with f_c and f_b in a practical RAKE receiver. Table 6.1 - 6.5 shows the capacity, the required E_b / N_o for a given P_b and the bandwidth efficiency η which was expressed in Eq.3.5.1.1.2 for several operating conditions.

In order to compute the capacity for multicell, the parameters in Eq. 3.4.2.3 take the following values [32]:

d : effective voice duty cycle = 0.5
f_u : uplink frequency reuse efficiency = 0.65
S : number of angular sectors in a cell = 3

We observe that as f_c / f_b increases, the required E_b / N_o for a constant P_b increases and η decreases. This effect becomes more pronounced as the bandwidth and/or P_b decreases.

Table 6.1 Capacity and Efficiency for f_c = 1 MHz, f_d=0, and for $P_b=10^{-2}$

f_b (Kbps)	10	20	50
M	100	50	20
E_b/N_o (dB)	6.04	6.19	6.53
N (single)	24	12	4
N (multicell)	97	46	17
η (bps/Hz/user)	0.25	0.24	0.22

Table 6.2 Capacity and Efficiency for f_c = 1 MHz, f_d=0, and for P_b=10^{-3}

f_b (Kbps)	10	20	50
M	100	50	20
E_b/N_o (dB)	8.72	8.90	9.76
N (single)	13	6	2
N (multicell)	52	25	8
η (bps/Hz/user)	0.13	0.13	0.11

Table 6.3 Capacity and Efficiency for f_c = 2 MHz, f_d=0, and for P_b=10^{-2}

f_b (Kbps)	10	20	50
M	200	100	40
E_b/N_o (dB)	6.70	6.77	6.98
N (single)	42	21	8
N (multicell)	167	81	31
η (bps/Hz/user)	0.21	0.21	0.20

Table 6.4 Capacity and Efficiency for f_c = 2 MHz, f_d=0, and for P_b=10^{-3}

f_b (Kbps)	10	20	50
M	200	100	40
E_b/N_o (dB)	9.32	9.42	9.81
N (single)	23	11	4
N (multicell)	91	44	16
η (bps/Hz/user)	0.12	0.11	0.10

Table 6.5 Capacity and Efficiency for f_c = 2 MHz, f_d=0, and for P_b=10^{-4}

f_b (Kbps)	10	20	50
M	200	100	40
E_b/N_o (dB)	11.02	11.23	12.00
N (single)	15	7	2
N (multicell)	63	29	9
η (bps/Hz/user)	0.08	0.08	0.06

6.2.4 The Effect of Estimator LPF Bandwidth

Fig. 6.5 and Fig. 6.6 illustrate the effect of the channel parameter estimation noise for f_c = 1 and 2 MHz, f_b= 20 Kbps. We know that the estimator LPF bandwidth is proportional to the Doppler spread of the channel. It is noted that the change in P_b is insignificant when f_d is increased from 0 to 60 Hz which should be more than sufficient for a mobile speed of 50 km/hr. As shown in Fig. 6.5 and Fig. 6.6, the increase in P_b with f_d is somewhat less for f_c = 1 MHz.

6.2.5 The Effect of TDL Length

The effect of TDL is investigated on the RAKE receiver performance. Fig. 6.7 and Fig. 6.8 show the dependency of P_b on the number of taps of the receiver for f_c = 1 and 2 MHz. We assume that f_d = 60 Hz, f_b = 20 Kbps and E_b / N_o = 3, 6 and 10 dB. It can be seen that using a length which spans only half of the impulse response i.e., 3.8 μsec should be sufficient since more taps cannot provide significant additional gain and in practical systems, increases receiver complexity. From the figures it is also noted that the rate of change of the curve increases as E_b / N_o increases.

6.2.6 The Fluctuations in the Probability of Bit Error

Fig. 6.9 and Fig. 6.11 show the P_b versus profile number for f_c = 1 and 2 MHz. It is assumed that fd = 0, fb = 20 Kbps and E_b/N_o = 6.15 and 6.7 dB for f_c = 1 and 2 MHz respectively. It has been observed that P_b changes although perfect power control was assumed in simulations. These curves on the figures can also be interpreted as the local P_b versus time for a vehicle in motion. It is seen that the fluctuations on P_b become more pronounced as the bandwidth decreases since the diversity is more effective for larger bandwidths which causes a stable performance. The average, maximum and minimum of the P_b for 2 MHz are 0.01, 0.016, 0.0018 respectively. For 1 MHz, they are 0.01, 0.021, 0.0025.

The histograms in Fig. 6.10 and Fig. 6.12 depicts the relative frequency of the P_b for this simulation run. It should be noted that the values correspond to uncoded transmission and considerable improvement of P_b is possible. For example, using R = 3/4 convolutional codes with a constrained length of 8, a probability of bit error of about 10^{-5} can be reached.

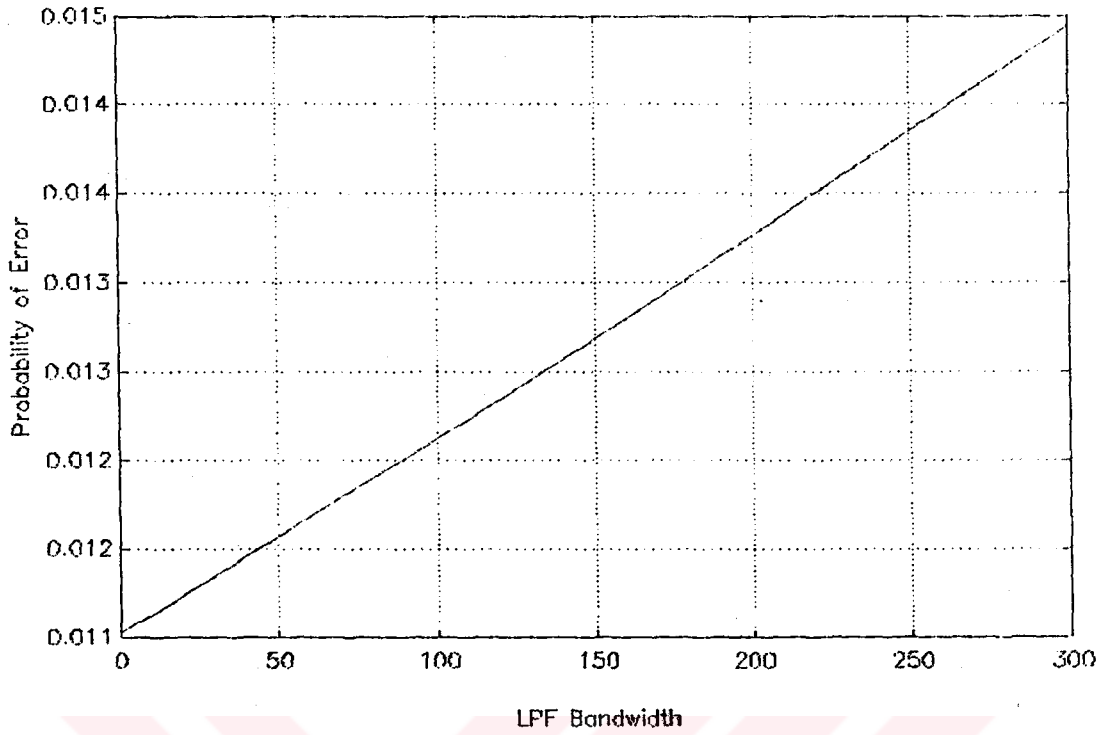

Figure 6.5. P_b vs. Estimator LPF Bandwidth, f_c=1 MHz, f_b=20 Kbps

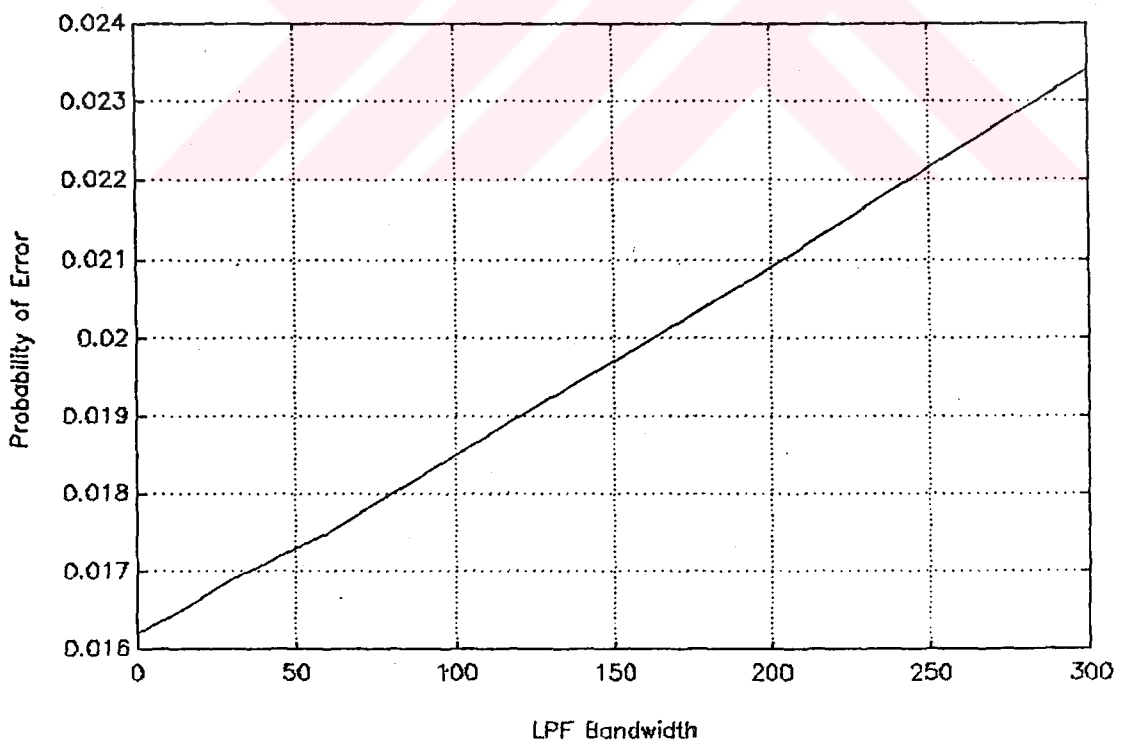

Figure 6.6. P_b vs. Estimator LPF Bandwidth, f_c=2 MHz, f_b=20 Kbps

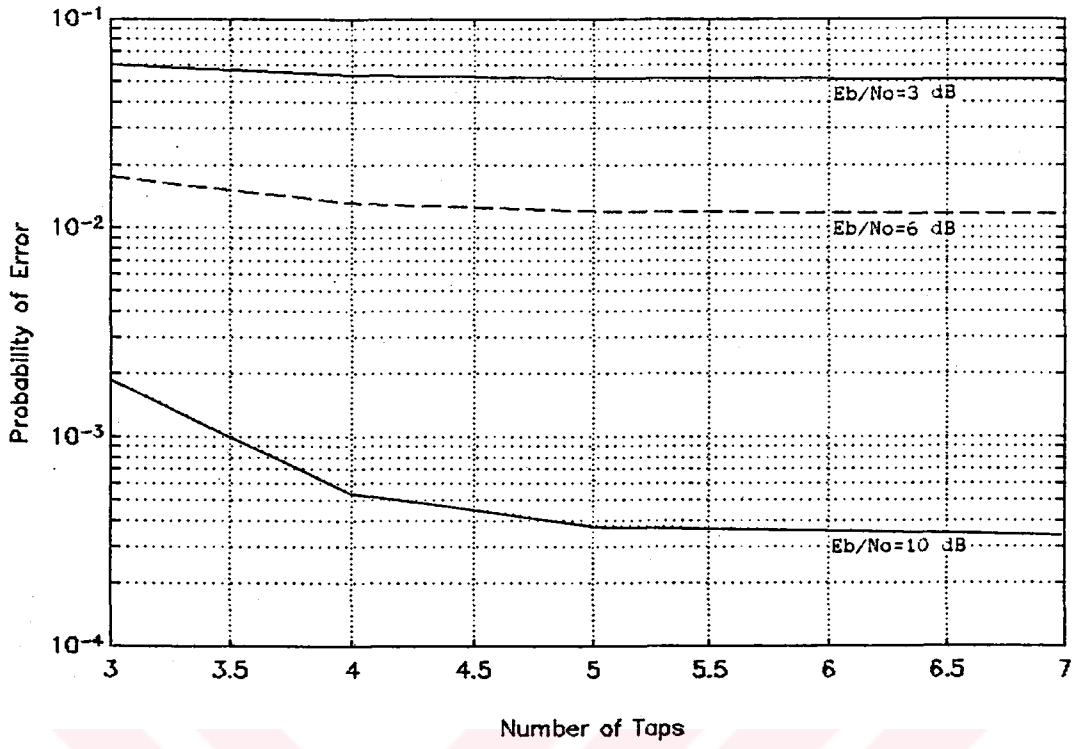

Figure 6.7. P_b vs. Number of Taps for f_c=1 MHz, f_d=60, f_b=20 Kbps

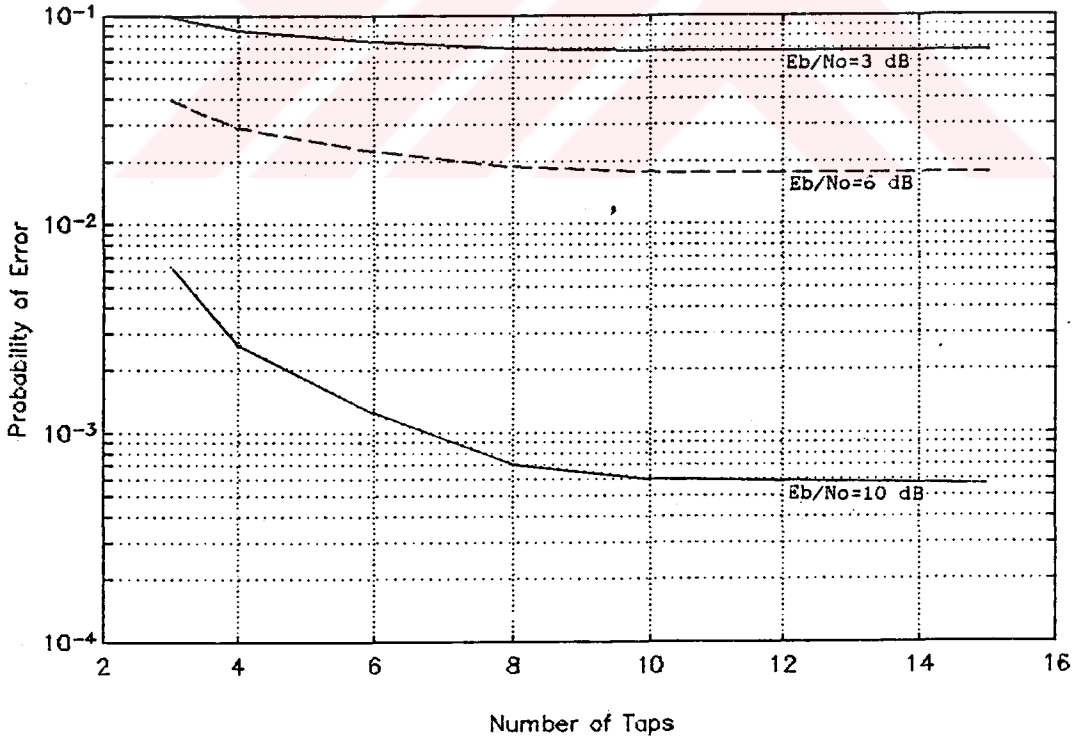

Figure 6.8. P_b vs. Number of Taps for f_c=2 MHz, f_d=60, f_b=20 Kbps

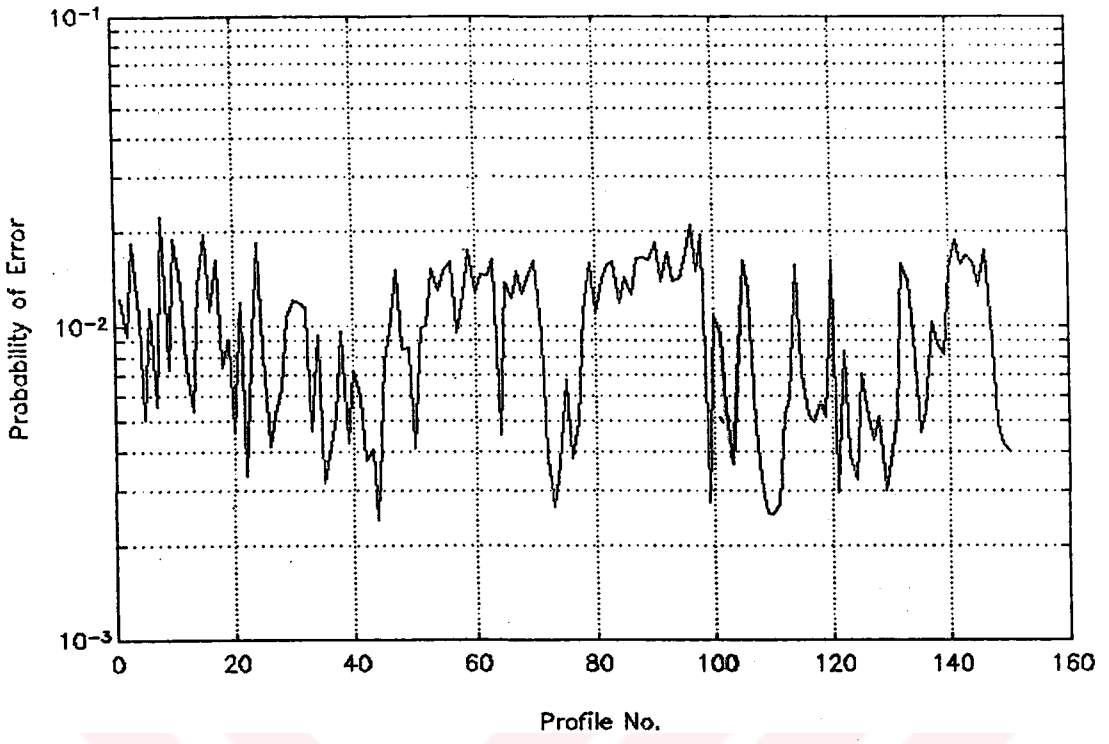

Figure 6.9. P_b vs. Profile Number for f_c=1 MHz, f_d=0, f_b=20 Kbps, E_b/N_o=6.15 dB

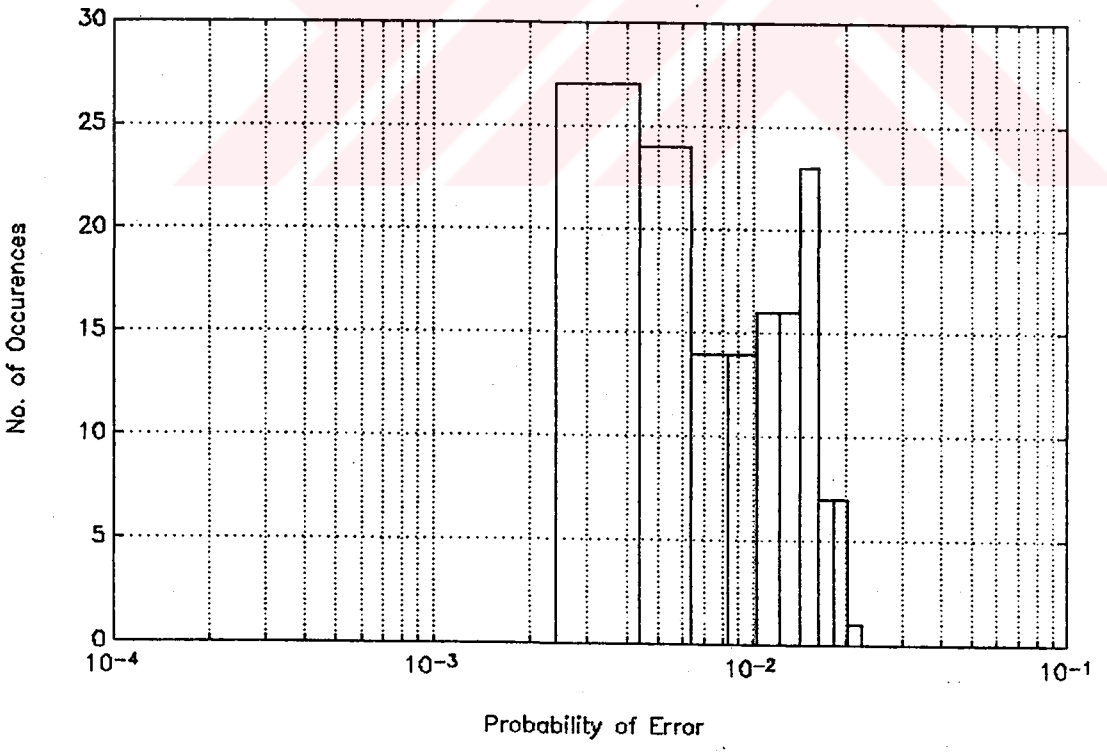

Figure 6.10. Number of Occurences vs. P_b, f_c=1 MHz, f_d=0, f_b=20 Kbps, E_b/N_o= 6.15 dB

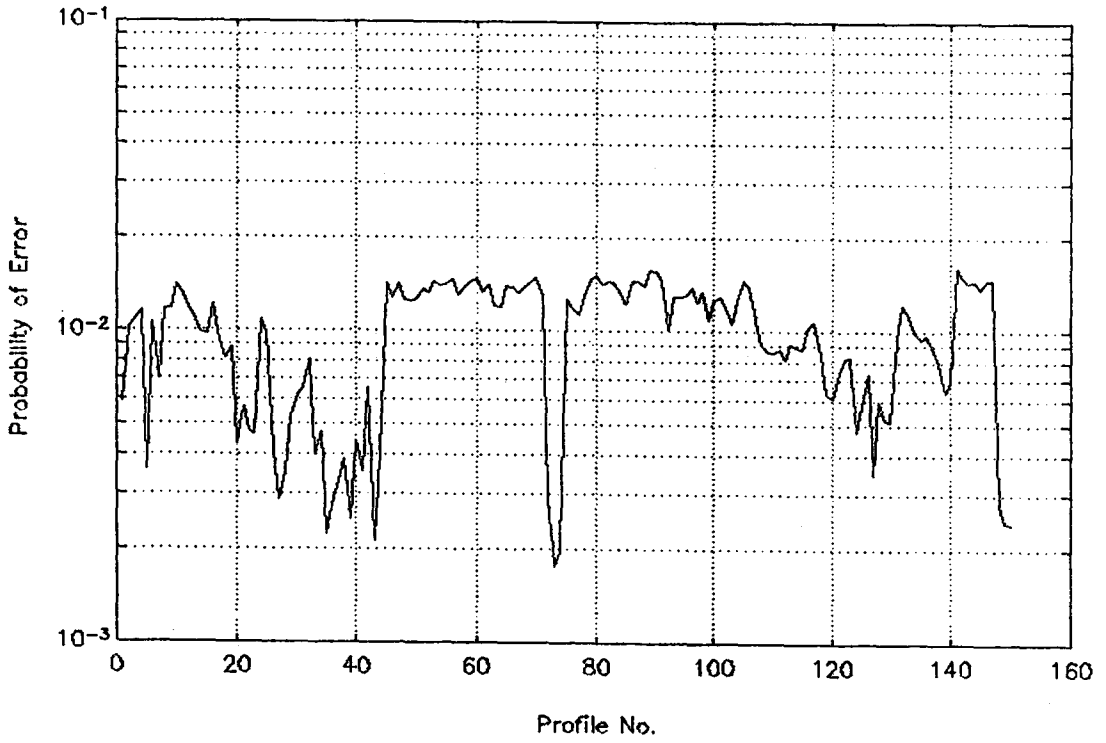

Figure 6.11. P_b vs. Profile Number for f_c=2 MHz, f_d=0,f_b=20 Kbps, E_b / N_o = 6.7 dB

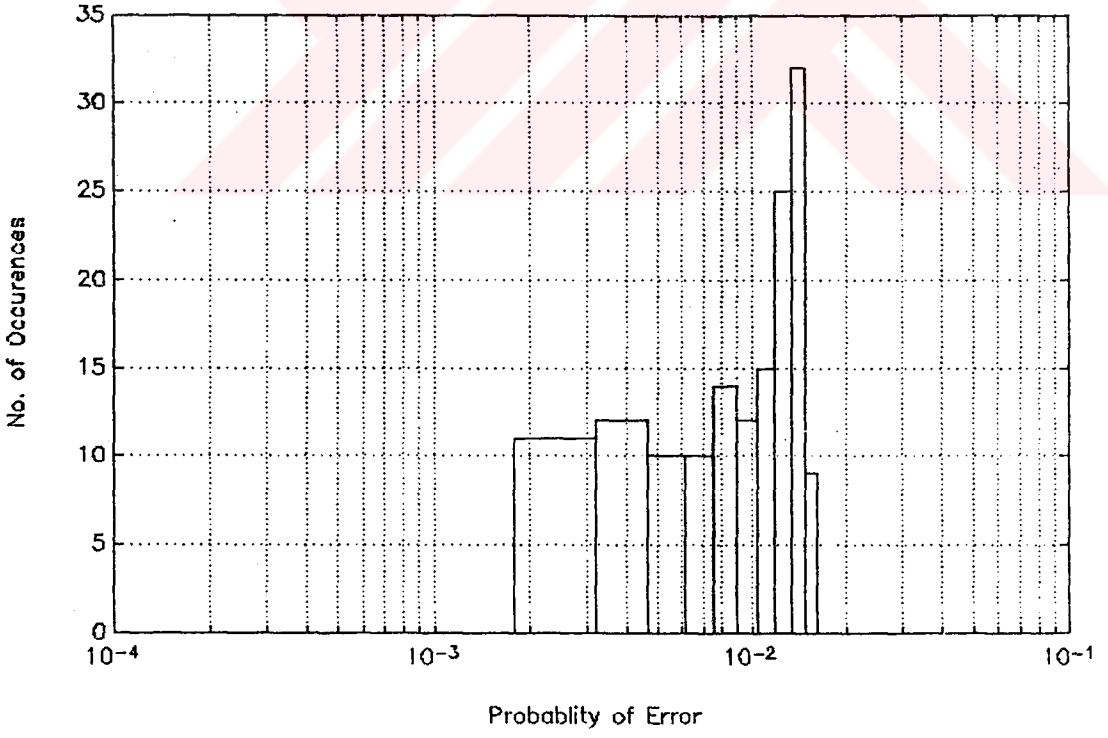

Figure 6.12. Number of Occurences vs. P_b, f_c=2 MHz, f_d=0, f_b=20 Kbps, E_b/N_o=6.7 dB

CHAPTER VII

CONCLUSIONS

In this thesis, the aim was to investigate the performance of RAKE receiver with BPSK data modulation for CDMA systems using a realistic channel model. The RAKE receiver was implemented with the maximal ratio combiner (MRC) using the estimated channel parameters as its weights. The Suzuki-Hashemi channel model was used in simulations. The probability of bit error was calculated under several operating conditions: Combinations of different E_b / N_o, slow and perfect power control, bit rate, Doppler spread, number of taps of the RAKE receiver were considered. Using these parameters, the capacity of CDMA spread spectrum were evaluated. Fluctuations of the probability of bit error were also observed, although perfect power control was assumed in simulations.

There are still disagreements between different researches regarding to channel model. For example, in Hashemi's channel model, paths are assumed to be correlated, lognormal processes, whereas in the COST 207 model, they are taken as independent, Rayleigh processes. This subject continues to be a challenging research topic.

Perfect timing and synchronization of the carrier were assumed in simulations. However, in practical systems, these assumptions are not strictly valid. In our analyses, the bandwidth of the pulse shaping filter was assumed to be very near to the required minimum bandwidth for data transmission. As a result of this, the channel tap spacing was taken to be T_c. Nevertheless, in practical systems, some amount of excess bandwidth is necessary for data transmission. Therefore, for a realistic channel model, the spacing should be equal to $T_{c/2}$ [9] and this gives rise to the problem of sensitivity of the system performance due to the sampler clock' s phase.

In our model, we used an I-Q detector in the RAKE receiver with perfect carrier synchronization. However, when perfect carrier synchronism is not possible, the phase of the estimated channel parameters will rotate. If this rotation is too fast, the estimator LPF bandwidth should increase. Thus, the noise level (including AWGN and interferences) also increases, which causes the degradation of the system performance. Hence, it seems that there is a need for a carrier synchronizer so that the frequency differences between the transmitter and the receiver can be kept reasonably small.

In addition, spreading sequence (ss) synchronization was assumed in our analyses. Because of the RAKE receiver structure, the receiver processes any signal component that falls in its span. It is obviously necessary to scan the channel impulse response by varying the ss phase. Then, the receiver's ss phase can be adjusted according to the channel impulse response, where the strongest paths are available.

As a result, subjects related to synchronization and timing should be taken into account for a more realistic performance evaluation.

The sum of the interferences from other users has been assumed to be Gaussian distributed. This assumption is also found in the literature [5,6,16,17]. Especially, at very low bit error rates, the tail of the Gaussian distribution has to be considered. If the number of users is low (5-10), this assumption may be invalid in these regions. However, at high or moderate bit error rates, Gaussian distribution is reasonably applicable.

In our simulations, the spreading sequences were considered to be perfect random sequences, whereas in reality, they are pseudorandom (PN) sequences. The moments of orders greater than two of PN sequences depend on the specific PN generator's topology and they are different than those of a truly random binary sequence. Since higher orders appear in our analyses, the results will be affected accordingly.

It is noted that we assumed the availability of data sequence at the receiver which is possible only in training portions of data. However, in practical systems , a decision feedback mechanism is used to supply the necessary data signal at the receiver. Therefore,some noise due to erroneous detection is introduced, but this is not

taken into account in our model. Hence, the performance is expected to be lower. If the probability of bit error is small enough ($P_b<10^{-2}$) during actual data transmission portions, the effect of this noise is thought to be very small. However, if we work in a region where the probability of bit error is around 10^{-1}, the performance should be affected considerably.

As mentioned earlier, BPSK modulation is used in this work, but in future works, more efficient modulation schemes, like QPSK may be investigated. In addition, the short term orthogonality properties of pseudorandom (PN) sequences will have to be considered. For example,the signal, before transmission, may be modulated again by using a binary orthogonal code (based on Walsh transform functions) as used in QUALCOMM's system [32]. Furthermore, suitable error correction coding schemes should be investigated in conjunction with the analysis on the gross probability of bit error.

Finally, we hope that more realistic performance assessments will be possible as the researches on the channel modeling provide better results.

REFERENCES

[1] H. Hashemi, "Simulation of a Urban Radio Communication Channel", Ph. D. thesis, Dept. of Elect. Eng. Comput. Sci., Univ. California, Berkeley, Aug. 1977.

[2] H. Hashemi, "Simulation of the Urban Radio Propagation Channel", IEEE Trans. on Veh. Tech. , vol. VT-28, pp. 213-224, Aug 1979.

[3] H. Suzuki, "A Statistical Model for Urban Radio Propagation Channel", Doctoral Dissertation, Univ. California, Berkeley, 1975.

[4] H. Suzuki, "A Statistical Model for Urban Radio Propagation Channel", IEEE Trans. on Commun., vol. COM-25, pp. 673-680, July 1977.

[5] G.L. Turin, "Introduction to Spread-Spectrum Antimultipath Technics and Their Application to Urban Radio", IEEE Proceedings, vol. 68, No. 3, pp. 328-353, March 1980.

[6] G.L. Turin, "The Effects of Multipath and Fading on the Performance of Direct Sequence CDMA Systems", IEEE J. Selected Areas Commun., vol. SAC-2. pp. 597-603, July 1984.

[7] G.L. Turin, et al. "A Statistical of Urban Multipath Propagation", IEEE Trans. on Veh. Tech., vol. VT-21, pp. 1-9, Feb. 1972.

[8] K. Pahlavan and Matthews, "Performance of Adaptive Matched Filter Receivers Over Fading Multipath Channels", IEEE Trans. Commun., vol. 38, No. 12, pp. 2106-2113, Dec 1990.

[9] J. G. Proakis, Digital Communications, 2nd Ed., McGraw-Hill, 1989.

[10] G.R. Copper and R.W. Nettleton, "A Spread-Spectrum Technique for high capacity mobile communications", IEEE Trans. on Veh. Tech., vol. VT-27, No. 4, pp. 264-275, Nov. 1978.

[11] A.A.M. Saleh and R.A. Valenzuala, "A Statistical Model for indoor multipath propagation", IEEE Selected Areas Commun., vol. 5, No. 2, pp. 128-137, Feb. 1987.

[12] A. Salamasi, "An Overview of Code Division Multiple Access (CDMA) Applied to the Design of Personal Communications Networks", Proceedings of the 2nd Rutgers University WINLAB Workshop on 3rd Generation Wireless Information Networks, East Brunswick, New Jersey, October 18-19 1990.

[13] U. Grob. et al., "Microcelluar Direct-Sequence Spread-Spectrum Radio System Using N-Path RAKE Receiver", IEEE Selected Areas on Commun., vol. 8, pp. 772-780, June 1990.

[14] P.W. Baier and P. Jung , "Potential an Limitations of CDMA and Spread-Spectrum Techniques in Cellular Mobile Radio Applications", COST 231 TD-012, Florence, January 1991.

[15] R.A. Iltis, "Joint Estimation of PN Code Delay and Multipath Using the Extended Kalman Filter", IEEE Trans. Commun., vol. 38, pp. 1672-1685, Oct. 1990.

[16] K. Yao, "Error Probability of Asynchronous Spread-Spectrum Multiple-Access Communication Systems", IEEE Trans. Commun., vol. COM-25, pp. 803-809, August 1977.

[17] J.E. Mazo, "Some Theoretical Observations on Spread-Spectrum Communications", Bell Syst. Tech. J., vol. 58, pp. 2013-2033, Nov. 1979.

[18] R.E. Ziemer and R.L. Peterson, Digital Communications and Spread Spectrum System, MacMillan, New York, 1985.

[19] G.C. Clark, Jr., and J.B. Cain, Error-Correction Coding for Digital Communications, Plenum Press, New York, 1981.

[20] A. Papoulis, Probability, Random Variables, and Stochastic Process, 2nd Ed., McGraw-Hill,1984.

[21] COST 207, Digital Land Mobile Radio Communications, Final Report,Commission of the European Communities, 1989.

[22] Simon, et al., Spread Spectrum Communications, vol. 3, Computer Science Press Inc., 1985

[23] W.C.Y. Lee, Mobile Cellular Telecommunications Systems, McGraw-Hill, 1989.

[25] H. Ochsner," Overview of the Radio Subsystem", CEPT/GSM-PN, Paris, France.

[26] D.J. Goodman, "Trends in Cellular and Cordless Communications", IEEE Communications Magazine, pp. 31-40, June 1991.

[27] S.C. Gupta, R. Viswanathan, R. Muammar, "Land Mobile Radio Systems", IEEE Communications Magazine, vol. 23, No. 6, June 1985.

[28] J.S. Lehnert, M.B. Pursley, "Multipath Diversity Reception of Spread-Spectrum Multiple Access Communcations", IEEE Trans. on Commun., vol. 35, No. 11, November 1987.

[29] I.M. Jacobs, et al, CDMA for Cellular and Personal Communication Network: Theory and Achievements, Geneva Switzerland, Oct. 1991.

[30] Y. Tanık, A. Yanartaş and S. Koç, "Performance Assessment of a BPSK CDMA System Using an Urban Radio Channel Model", COST 231, MC Meeting, The Hague, Netherlands, Sep. 1991.

[31] D. L. Nielson, "Microwave Propagation and Noise Measurements for Mobile Radio Application", IEEE Trans. on Veh. Tech., vol. 21, pp. 9-16, Feb. 1972.

[32] A. Salmasi and K. S. Gilhousen, "On the System Design Aspects of Code Division Multiple Access (CDMA) Applied to Digital Cellular and Personal Communications Networks", IEEE Conference on Veh. Tech., 1991

APPENDICES

APPENDIX A

The computational procedures for the terms that appear in Eq. 5.2.2.33 and Eq. 5.2.2.34 will be explained in this Appendix.

The channel noise υ_i was rewritten in Eq.5.2.2.9 in Chapter 5. Since $\gamma_i(m)$ and $\eta_i(m)$, which were defined in Eq.5.2.2.10 and 5.2.2.11 respectively, are uncorrelated zero mean sequences, $\psi_{\upsilon_i\upsilon_j}(0)$ in Eq. 5.2.2.33 can be expressed by

$$\psi_{\upsilon_i\upsilon_j}(0) = \psi_{\gamma_i\gamma_j}(0) + \psi_{\eta_i\eta_j}(0) \tag{A-1}$$

Then, $\psi_{\gamma_i\gamma_j}(0)$ and $\psi_{\eta_i\eta_j}(0)$ are evaluated separately. $\psi_{\eta_i\eta_j}(0)$ is

$$\psi_{\eta_i\eta_j}(0) = \frac{1}{M^2}\sum_{r=0}^{M-1}\sum_{r'=0}^{M-1} E\left\{\mu_{mM+r+L_2-i}\,\mu^*_{mM+r'+L_2-j}\,p_{mM+r}\,p_{mM+r'}\right\} \tag{A-2}$$

Since $\{P_k\}$ and $\{\mu_k\}$ are uncorrelated, the expectations are are separated

$$\psi_{\eta_i\eta_j}(0) = \frac{1}{M^2}\sum_{r=0}^{M-1}\sum_{r'=0}^{M-1} E\left\{\mu_{mM+r+L_2-i}\,\mu^*_{mM+r'+L_2-j}\right\} E\left\{p_{mM+r}\,p_{mM+r'}\right\} \tag{A-3}$$

By using the fact that $E\{p_k p_l\} = 1$, if $k = l$, we have;

$$E\{p_{mM+r}\, p_{mM+r'}\} = \begin{cases} 1 & r = r' \\ 0 & \text{otherwise} \end{cases}$$

Hence, $\psi_{\eta_i\eta_j}(0)$ takes the form:

$$\psi_{\eta_i\eta_j}(0) = \frac{1}{M^2} \sum_{r=0}^{M-1} E\{\mu_{mM+r+L_2-i}\, \mu^*_{mM+r+L_2-j}\} \qquad \text{(A-4)}$$

Since $\{\mu_k\}$ is a zero mean uncorrelated sequence with $2N_0$ as its power spectral density,

$$E\{\mu_{k+l}\, \mu^*_k\} = 2N_0\delta_l \qquad \text{(A-5)}$$

Eq. (A-4) becomes

$$\psi_{\eta_i\eta_j}(0) = \frac{1}{M} 2N_0\delta_{ij} \qquad \text{(A-6)}$$

Next we consider $\psi_{\gamma_i\gamma_j}(0)$. Making use of the assumptions made earlier in Chapter 5, $\psi_{\gamma_i\gamma_j}(0)$ is

$$\psi_{\gamma_i\gamma_j}(0) = \frac{1}{M^2} \sum_{\substack{l=0 \\ l\neq L_2-i}}^{L} \sum_{\substack{l'=0 \\ l'\neq L_2-i}}^{L} \beta_l\, \beta^*_{l'} \sum_{r=0}^{M-1} \sum_{r'=0}^{M-1} E\left\{d\left[\frac{mM+r+L_2-i-l}{M}\right] d\left[\frac{mM+r'+L_2-j-l'}{M}\right]\right\}$$

$$*E\{p_{mM+r+L_2-i-l}\, p_{mM+r}\, p_{mM+r'+L_2-j-l'}\, p_{mM+r'}\}$$

(A-7)

Like $\phi_{\vartheta_i\vartheta_j}(0)$ in Eq. 5.2.2.16, the same case by case procedure is applied to determine the the expected value of the product of four binary random variables. The pairwise equations are checked by examining the indices of $\{p_k\}$. The result for $\psi_{\gamma_i\gamma_j}(0)$ is

$$\psi_{\gamma_i\gamma_j}(0) = \frac{1}{M} \sum_{\substack{l=0 \\ l\neq L_2-i}}^{L} \beta_l \beta^*_{l+i-j} + \frac{1}{M^2} \sum_{\substack{l=0 \\ l\neq L_2-i}}^{L} \beta_l \beta^*_{2L_2-i-j-l}\, b(L_2-i-l) \quad \text{(A-8)}$$

where b(.) was determined in Eq.5.2.2.18

By using Eq. (A-6) and Eq. (A-8), Eq. 5.2.2.33 is obtained.

Now, $\psi^*_{a_ia_j}$ in Eq. (5.2.2.34) is considered.

Let $x_i(m) = \upsilon_i(m)dm$. By following the same procedure, used in calculating $\phi_{a_ia_j}(0)$, in Eq. (5.2.2.21), we have:

$$\psi^*_{a_ia_j}(0) = 2f_d T_b \sum_k \psi^*_{x_ix_j}(k) \quad \text{(A-9)}$$

Now, $\psi^*_{x_ix_j}(k)$ should be found. Let $x_i(m) = \gamma_i(x)+\eta_i(m)$ where $\gamma_i(m)$ and $\eta_i(m)$ were defined in Eq. 5.2.2.24 and Eq. 5.2.2.25, respectively. Since they are uncorrelated sequences, $\psi^*_{x_ix_j}(0)$ becomes;

$$\psi^*_{x_ix_j}(k) = \psi^*_{\eta_i\eta_j}(k) + \psi^*_{\gamma_i\gamma_j}(k) \quad \text{(A-10)}$$

First, $\psi^*_{\eta_i\eta_j}(k)$ is evaluated.

$$\psi^*_{\eta_i\eta_j}(k) = \frac{1}{M^2}\sum_{r=0}^{M-1}\sum_{r'=0}^{M-1} E\left\{\mu^*_{(m+k)M+r+L_2-i}\,\mu_{mM+r'+L_2-j}\right\}$$

$$* E\left\{d_{(m+k)}\,d_m\right\} E\left\{p_{(m+k)M+r}\,p_{mMr'}\right\} \qquad \text{(A-11)}$$

By using the conditions which were defined for Eq. 5.2.2.27 in Chapter 5, $\psi^*_{\eta_i\eta_j}(k)$ is

$$\psi^*_{\eta_i\eta_j}(k) = \frac{1}{M^2}\sum_{r=0}^{M-1} E\left\{\mu^*_{mM+r+L_2-i}\,\mu_{mM+r+L_2-j}\right\}\delta_k \qquad \text{(A-12)}$$

Considering Eq. (A-5), $\psi^*_{\eta_i\eta_j}(k)$ becomes

$$\psi^*_{\eta_i\eta_j}(k) = \frac{1}{M}2N_0\delta_{ij} \qquad \text{(A-13)}$$

Now, we should find $\psi^*_{\gamma_i\gamma_j}(k)$.

By the same procedure used to calculate $\phi_{\gamma_i\gamma_j}(k)$ in Eq. 5.2.2.29, $\psi^*_{\gamma_i\gamma_j}$ is given as:

$$\psi^*_{\gamma_i\gamma_j}(k) = \frac{1}{M}\sum_{\substack{l=0\\ l\neq L_2-i}}^{L}\beta_l^*\,\beta_{l+i-j}\,\delta_k + \frac{1}{M^2}\sum_{\substack{l=0\\ l\neq L_2-i}}^{L}\beta_l^*\,\beta_{2L_2-i-j-l}\,b(kM+L_2-i-l) \qquad \text{(A-14)}$$

Finally, we get Eq. 5.2.2.34 by using Eq. (A-13) and Eq. (A-14).

APPENDIX B

This program is developed to investigate the probability of error of the system that is defined in this thesis. The program is in Pascal and developed in Turbo Pascal enviroment (Turbo Pascal is trademark of Borland International, Inc.). It makes use of the library routines supplied together with the Turbo Pascal compiler.

```
PROGRAM ERROR;

{   This program uses Hashemi-Suzuki channel simulation results.
 Then,noise variance and probability of error are calculated
 for given channel parameters.}

 {$N+}

 USES
   Graph,crt,utility;

 TYPE
   complex  = record
    re,im: single;
 end;

 CONST
   czero: complex = (re:0; im:0);

 VAR
   NoOfTaps,ChipsPerBit,NoOfProfiles : Integer;
   bx                          : Array [-1000..1000] of Integer;
   AVPG,E,TB,FD,NO,PE,PE1,EN         : Single;
   BETA                          : Array [0..75] of Complex;


 PROCEDURE   Cadd( x,y: Complex ; Var z: Complex);

   Begin
     z.re:=x.re+y.re;
     z.im:=x.im+y.im;
   End;

PROCEDURE CMult( x,y: Complex; Var z: Complex);

  Begin
    z.re:=x.re*y.re-x.im*y.im;
```

```
    z.im:=x.re*y.im+x.im*y.re;
  End;

PROCEDURE Conj( x: Complex; Var y: Complex);

  Begin
     y.re:=x.re; y.im:= -x.im;
  End;

PROCEDURE AV(I,J: Integer; Var PHIA,PHIV,PSIA,PSIV: Complex);

  Var
    bxx,ll,kk,tl2                                          : Integer;
    sumH1,sumH2,sumH3,sumS1,sumS2,sumS3,LPSIA,LPSIV,z: Complex;
    sumH1D,sumH2D,sumH3D,sumS1D,sumS2D,sumS3D          : Complex;
  Begin
    sumh1:=czero;
    sumH2:=sumH1;
    sumH3:=sumH1;
    sumS1:=sumH1 ;
    sumS2:=sumH1 ;
    sumS3:=sumH1 ;

    For  LL:=0 to NoOfTaps do
      Begin
        bxx := bx[ NoOfTaps-I-LL ];
        If (bxx=-999) Then
          write( 'ARRAY ELEMENT IS NOT CALCULATED');
        If ((LL<>NoOfTaps-I) And ((0<=LL+I-J) And
                              (LL+I-J<=NoOfTaps))) Then
           Begin
             cmult(beta[ll],beta[ll+i-j],z);
             cadd(sumh1,z,sumh1);
             conj(beta[ll],z);
             cmult(z,beta[ll+i-j],z);
             cadd(sums1,z,sums1);
           End;
        If ((LL<>NoOfTaps-I) And ((0<=2*NoOfTaps-I-J-LL)
                    And (2*NoOfTaps-I-J-LL<=NoOfTaps))) Then
           Begin
             cmult(beta[ll],beta[2*NoOfTaps-i-j-ll],z);
             z.re:=bxx*z.re;
             z.im:=bxx*z.im;
             cadd(sumh3,z,sumh3);
             conj(beta[2*NoOfTaps-i-j-ll],z);
             cmult(beta[ll],z,z);
             z.re:=bxx*z.re;
             z.im:=bxx*z.im;
             cadd(sums3,z,sums3);
           End{if};
      End {ll};

      For kk:=-1 to 1 do
        For ll:=0 to NoOfTaps do
          Begin
```

```
TL2:=2*NoOfTaps-I-J-LL;
bxx:=bx[KK*ChipsPerBit+NoOfTaps-I-LL];
If (bxx=-999) Then
  Begin
    Write('ARRAY ELEMENT IS NOT CALCULATED');
    Write('ELEMENT NO(KK*ChipsPerBit+NoOfTaps-I-LL)'
                    , KK*ChipsPerBit+NoOfTaps-I-LL);
    Write( 'KK = ',KK);
    Write( 'ChipsPerBit  = ',ChipsPerBit);
    Write( 'NoOfTaps = ',NoOfTaps);
    Write( 'I  = ',I);
    Write( 'LL = ',LL );
    Readln;
  End;

  If ((LL<>NoOfTaps-I) And ((0<=TL2) And
                      (TL2<=NoOfTaps))) Then
    Begin
      CMmult(beta[ll],beta[tl2],z);
      z.re:=bxx*z.re;
      z.im:=bxx*z.im;
      Cadd(sumh2,z,sumh2);
      Conj(beta[ll],z);
      CMult(z,beta[tl2],z);
      z.re:=bxx*z.re;
      z.im:=bxx*z.im;
      Cadd(sums2,z,sums2);
      End {IF};
    End;

    sumh2d.re:=sumh2.re/ChipsPerBit/ChipsPerBit;
    sumh2d.im:=sumh2.im/ChipsPerBit/ChipsPerBit;
    sumh1d.re:=sumh1.re/ChipsPerBit;
    sumh1d.im:=sumh1.im/ChipsPerBit;
    Cadd(sumh1d,sumh2d,z);
    z.re:=2*fd*tb*z.re;
    z.im:=2*fd*tb*z.im;
    phia:=z;
    sumh3d.re:=sumh3.re/ChipsPerBit/ChipsPerBit;
    sumh3d.im:=sumh3.im/ChipsPerBit/ChipsPerBit;
    sumh1d.re:=sumh1.re/ChipsPerBit;
    sumh1d.im:=sumh1.im/ChipsPerBit;
    Cadd(sumh1d,sumh2d,z);
    phiv:=z;
    sums2d.re:=sums2.re/ChipsPerBit/ChipsPerBit;
    sums2d.im:=sums2.im/ChipsPerBit/ChipsPerBit;
    sums1d.re:=sums1.re/ChipsPerBit;
    sums1d.im:=sums1.im/ChipsPerBit;
    Cadd(sums1d,sums2d,z);
    z.re:=2*fd*tb*z.re;
    z.im:=2*fd*tb*z.im;
    lpsia:=z;
   if i=j then
     lpsia.re:=lpsia.re+4*fd*tb*n0/ChipsPerBit;
   psia:=lpsia;
```

```
                sums3d.re:=sums3.re/ChipsPerBit/ChipsPerBit;
                sums3d.im:=sums3.im/ChipsPerBit/ChipsPerBit;
                conj(sums1,z);
                z.re:=z.re/ChipsPerBit;
                z.im:=z.im/ChipsPerBit;
                Cadd(z,sums3d,lpsiv);
                if i=j then
                lpsiv.re:=lpsiv.re+2*n0/ChipsPerBit;
                psiv:=lpsiv;
    End;

PROCEDURE PSIPHI(I,J:integer;Var PSIW,PHIW:complex);
  Var
    w,z,PHIAIJ,PHIVIJ,LPHIW,PSIAIJ,PSIVIJ,LPSIW : complex;
  Begin
    AV(I,J,PHIAIJ,PHIVIJ,PSIAIJ,PSIVIJ);
    CMult(beta[NoOfTaps-i],beta[NoOfTaps-j],lphiw);
    conj(phiaij,z);
    CMult(lphiw,z,lphiw);
    conj(beta[NoOfTaps-i],z);
    conj(beta[NoOfTaps-j],w);
    CMult(z,w,w); cmult(w,phivij,w);
    lphiw.re := lphiw.re +w.re;
    lphiw.im := lphiw.im +w.im;
    conj(phiaij,z);
    CMult(z,phivij,z);
    Cadd(z,lphiw,lphiw);
    PHIW:=LPHIW;
    conj(beta[NoOfTaps-j],z);
    CMult(beta[NoOfTaps-i],z,z);
    CMult(psiaij,z,lpsiw);
    conj(beta[NoOfTaps-i],z);
    CMult(beta[NoOfTaps-j],z,z);
    CMult(z,psivij,z);
    Cadd(z,lpsiw,lpsiw);
    CMult(psiaij,psivij,z);
    Cadd(z,lpsiw,lpsiw);
    PSIW:=LPSIW;
  End;

FUNCTION BXY (k,ChipsPerBit : Integer) : Integer;
  Var
    r,sum : Integer;
  Begin
    sum:=0;
    for r:=0 to ChipsPerBit-1 do
    if (r+k>=0) and (r+k<=ChipsPerBit-1) then inc(sum);
    bxy:=sum;
  End;

FUNCTION ERFCC(x:double) : Double;
  Var
    t,erf1,erf2,erf3,erf4,erf5,erf6,erf7,z : Double;
  Begin
    z:=Abs(x);
```

```
    t:=1./(1.+ 0.5*Z);
    erf1:=T*(-0.82215223+T*0.17087277);
    erf2:=T*(-1.13520398+T*(1.48851587+erf1));
    erf3:=T*(-0.18628806+T*(0.27886807+erf2));
    erf4:=T*(1.00002368+T*(0.37409196+T*(0.09678418+erf3)));
    erf5:=-Z*Z-1.26551223+erf4;
    erf6:=Exp(erf5);
    erf7:=T*erf6;
    If (x<0) Then erfCC:=2.-erf7  Else  Erfcc := erf7;
  End;


        {   Probability of Error for ideal channel    }

PROCEDURE PEB(EN:single;var PE1:single);
  Var
    w : double;
  Begin
    w:=sqrt(en);
    pe1:=erfcc(w);
    pe1:=pe1*0.5;
  End;

   VAR
     Tap1,Tap2      : Integer;
     stres          : String;
     infile1        : File of Extended;
     infile2        : File of Single;
     st1,st2        : String;
     psiwij,phiwij  : Complex;


              {Probability of Error}

PROCEDURE PEERR(E:single;var PE:single);
  Var
    i:integer;
    y,sum,w:single;
    z:complex;
  Begin
    sum:=0.;
    For i:=Tap1 to Tap2 do
          sum:= sum + sqr(beta[NoOfTaps-i].re)
                + sqr(beta[NoOfTaps-i].im);
    y:=sqrt(2.*e);
    pe:=0.5*erfcc(sum/y);
  End;

 VAR
   vr,PeAvg : Extended;
   sum,sum1 : Extended;
   EnDB     : Single;
   i,j,k    : Integer;
   fil      : Text;
```

```
            {    main program     }

Begin
  Clrscr;
  WriteLn('RAKE RECEIVER PERFORMANCE WITH POWER CONTROL');
  WriteLn; writeln;
  Write('FileName to read beta''s(*.MAT) =');
  readln(st2);
  Assign(fl1,st2+'.mat');
  Reset(fl1);
  Write('ENTER MaxNoOfTaps (<=75) : ');
  Read(NoOfTaps);
  Write( 'ENTER ChipsPerBit (M=Tb/Tc) : ');
  Read( ChipsPerBit);
  Write( 'ENTER fc : ');
  Read( TB);
  tb:=ChipsPerBit/tb;
  Write( 'ENTER FD : ');
  Read( FD);
  Write( 'ENTER EB/NO : ');
  Read( ENDB);
  Write( 'ENTER THE TOTAL NUMBER OF PROFILES (1 TO 150): ');
  Read( NoOfProfiles);
  Write('TAP-1 : ');
  Read(i);
  Write('TAP-2 : ');
  Read(Tap2);
  Write('FileName to store probability of error for
                                        prof.(*.DAT) =');
  Readln;
  Readln(st2);
  Assign(infile2,'.\DATA\'+st2+'.DAT');
  ReWrite(infile2);
  Tap1:=NoOfTaps-Tap2;
  Tap2:=NoOfTaps-i;
  en:=exp(endb/10*ln(10));
  PEB(EN,PE1);
  Writeln( 'PROBABILITY OF ERROR  FOR EB/NO (in db)',
                                      ENdB:6:1, ':', PE1);
  For i:=-1000 to 1000 do
    bx[I]:=-999;
  If ((-ChipsPerBit-NoOfTaps<-1000) Or
                  (ChipsPerBit+NoOfTaps>1000)) Then
    Begin
      Write( 'ARRAY DIMENSIONS WILL BE EXCEEDED');
      Halt;
    End;
  For I:=-ChipsPerBit-NoOfTaps-1 to ChipsPerBit+NoOfTaps+1 do
    bx[I]:=BXY(I,ChipsPerBit);
  PeAvg:=0;
  WriteLn('Profile No.      Probabilty of Error');
  For k:=1 to NoOfProfiles do
     Begin
```

```
        avpg:=0;
        For i:=0 to NoOfTaps do
          Begin
            Read(fl1,beta[i].re,beta[i].im);
            avpg:=avpg+sqr(beta[i].re)+sqr(beta[i].im);
          End;
        NO:=ChipsPerBit*avpg/2./EN;
        sum:=0;  sum1:=0;
        For i:= Tap1 to Tap2 do
          Begin
            For j:=i to Tap2 do
              Begin
                PSIPHI(I,J,PSIWIJ,PHIWIJ);
                If i=j Then
                  Begin
                    sum1:=sum1+PHIWIJ.re+PSIWIJ.re;
                  End Else
                  Begin
                    sum:=sum+2*PHIWIJ.re+2*PSIWIJ.re;
                  End;
                sum:=(sum1 + sum)*0.5;
              End; {j}
          End; {i}
        E:=sum;
        PEERR(E,PE);
        Writeln(k,'                ' ,PE);
        Write(infile2,pe);
        PeAvg:= PeAvg + Pe;
      end;  {Profiles}
      PeAvg:= PeAvg/NoOfProfiles;
  Writeln( 'PROBABILITY OF ERROR    :',PeAvg);
  Close(infile2);
  Close(fl1);
  Readln;
End.
```